The role of neurocranial shape in defining the boundaries of an expanded *Homo erectus* hypodigm

Karen L. Baab

Department of Anatomy, Arizona College of Osteopathic Medicine, Midwestern University, Glendale, AZ 85308, USA

A R T I C L E   I N F O

A B S T R A C T

The main goals of this study were to evaluate the distinctiveness of *Homo erectus* neurocranial shape relative to other closely related species, and assess the likelihood that particular fossils were correctly attributed to *H. erectus* given how shape variation related to geography, time and brain size. This was accomplished through analyses of several sets of landmarks designed to maximize the fossil sample, including 24 putative *H. erectus* fossils. The question of taxonomic differentiation was initially assessed for the type specimen (Trinil II) and morphologically similar Sangiran fossils and subsequently for increasingly inclusive definitions of *H. erectus*. Results indicated that *H. erectus* fossils from China, Indonesia, Georgia and East Africa shared a neurocranial shape that was distinct from that of other Plio-Pleistocene *Homo* taxa, a pattern only partially accounted for by brain size. Early Indonesian *H. erectus* formed a morphological "bridge" between earlier and later populations assigned to *H. erectus* from Africa and Asia, respectively. These results were combined with discrete characters to create a more complete species definition for *H. erectus*. There were two notable exceptions to the general pattern of *H. erectus* uniqueness. The 0.8–1.0 Ma (millions of years ago) Daka calvaria from Ethiopia consistently grouped with mid-Pleistocene *Homo*, including Bodo and Kabwe, rather than African or Asian *H. erectus*. In addition, Daka also exhibited several traits derived for mid-Pleistocene *Homo*, and its scaling pattern mirrored mid-Pleistocene *Homo* rather than *H. erectus*. Daka may have belonged to an "advanced" *H. erectus* population close to the root of *Homo heidelbergensis sensu lato (s.l.)*, or to an early population of *H. heidelbergensis s.l.*. The 1.5 Ma KNM-ER 42700 specimen from Kenya exhibited a unique calvarial shape distinct from *H. erectus* despite the exclusion of problematic landmarks from the frontal bone. These unique aspects of shape were not present in two other subadult fossils, KNM-WT 15000 and D2700.

© 2015 Elsevier Ltd. All rights reserved.

1. Introduction

The taxonomic integrity and composition of *Homo erectus* has been the subject of continuous debate since the erection of *Pithecanthropus erectus* by Dubois (1894). The most restricted conception of *H. erectus* limits the species to fossils from Trinil and Sangiran on the island of Java (Schwartz, 2004), while the most inclusive definitions incorporate fossils typically assigned to the species from Asia, Africa and Georgia, as well as fossils commonly assigned to earlier *Homo* species (namely *Homo habilis* and *Homo rudolfensis*; Lordkipanidze et al., 2013). It has even been suggested that *H. erectus* is not a distinct taxon, and should be sunk into *Homo sapiens* (Wolpoff et al., 1994). Most workers ascribe to either a

single *H. erectus* species that includes fossils from Indonesia (including the younger Ngandong, Sambungmacan, and Ngawi fossils), China, East Africa, and possibly South Africa (e.g., Rightmire, 1990; Antón, 2003; Baab, 2008b), or restrict *H. erectus* to the Asian fossils and assign the African and probably the Georgian fossils to the less derived *Homo ergaster* (e.g., Wood, 1994; Rosas and Bermudez De Castro, 1998; Vekua et al., 2002). This plethora of views reflects different species definitions and interpretations of the evolutionary dynamics and relationships within *Homo* as well as the complexity of operationalizing species definitions in the paleontological record, all deeply entrenched systematics issues that are unlikely to be resolved by any single analysis (for additional reviews of *H. erectus* systematics, see Dunsworth and Walker, 2002; Antón, 2003; Baab, 2014). Yet, some of the debate also relates to whether *H. erectus* is a distinct taxon that can be defined relative to other closely related and morphologically similar species, and how

individual fossils or fossil samples relate to one another (based on patterns of variation and covariation).

Several studies have addressed the degree of variation within the broadly defined *H. erectus* hypodigm or the degree of difference among subsets of this sample corresponding to temporal/ geographic groupings or proposed species boundaries (Kidder and Durband, 2000, 2004; Villmoare, 2005; Terhune et al., 2007; Baab, 2008b). The results mostly (but not exclusively) support a single species interpretation, but it was clear that the pattern of within sample variation is complex. This study contributes to the current debate by: (1) evaluating whether neurocranial shape alone can be used to define and differentiate *H. erectus*, and (2) assessing how different samples/specimens assigned to *H. erectus* relate to each other and to other taxa in terms of vault shape. A related goal is to describe and visualize shape differences between *H. erectus* and other Plio-Pleistocene *Homo* taxa. The first goal is addressed by examining increasingly more inclusive definitions of *H. erectus sensu lato (s.l.)*, beginning with just the geochronologically older Asian fossils and ending with the most recent additions to the hypodigm from the Caucasus and East Africa. It is important to evaluate if these taxonomic assignments are correct as they collectively expand the temporal and spatial bounds of *H. erectus* and impact our understanding of the evolutionary history of this species.

Common sources of intraspecific craniometric variation include geography, diachronic evolutionary trends and allometric variation. The second goal is therefore evaluated by asking whether the pattern of morphological variation accords with the pattern of geographic, temporal and size (specifically endocranial volume) variation in the sample. In other words, are fossils that are similar in their geographic origin, geochronological age, and brain size more similar to one another than other fossils that are more distinct for these parameters? Operationally, these patterns can only be assessed on a broad scale as these three factors are not an exclusive list of variables impacting intraspecific variation. To a more limited extent, these patterns should also hold between species, such that earlier members of *H. erectus* will more closely resemble early *Homo* species than later and more derived species. However, the magnitude of interspecific differences may be greater, as species may diverge more strongly along these axes. Along these lines, a major divergence from observed geographic, temporal and allometric patterning may indicate a species-level distinction. Important insights regarding the taxonomic validity and composition of *H. erectus* should emerge from the integration of these results with previous studies based on qualitative morphological descriptions.

Morphological definitions of *H. erectus* rely heavily on both discrete cranial traits and aspects of cranial shape. However, it is possible to improve the qualitative descriptions of cranial shape using a geometric morphometric (GM) approach, which is specifically designed to preserve shape throughout the analysis. This allows for cranial shape to be treated as a continuous variable rather than a series of discrete traits. Multivariate evaluation of shape quantified by 3D landmarks avoids subjective decisions about which aspects of shape are distinct features by analyzing the shape of the cranium as a single, integrated unit. Further, it clarifies how aspects of shape co-vary within or between groups and how this patterning may correspond to taxonomic boundaries. Finally, a GM approach may better capture the relatively subtle aspects of shape that differentiate closely-related Plio-Pleistocene *Homo* species (rather than the more visually apparent differences between *H. erectus* and *H. sapiens*). Many species definitions for *H. erectus* focus on differentiating it from modern *H. sapiens* (Wood, 1984; Wolpoff et al., 1994), but including species that abut *H. erectus* closely in time and that are more similar morphologically than *H. sapiens* is a more conservative test of whether *H. erectus* cranial shape is unique.

There are, however, disadvantages inherent in a GM approach to defining species and assessing taxonomic assignments, and the application of shape information to alpha taxonomy has been criticized (Wood quoted in Switek, 2013). By evaluating overall cranial shape rather than individual aspects of shape, incomplete fossils are often excluded from the analysis, thus reducing sample sizes. Also, by focusing on principal components of shape variation, this study is biased in favor of large scale shape features rather than small-scale differences in localized morphological structures. Moreover, shape analyses are ill-suited for evaluating truly discrete characters that are present or absent because capturing discontinuous variation using a set of landmarks that must correspond across taxa remains challenging (Bookstein, 2002; Klingenberg, 2008; Polly, 2008; Gómez-Robles et al., 2011). Finally, similarity in shape reflects a variety of factors that may overprint a species-specific pattern, including scaling effects and sexual dimorphism. Therefore, the information obtained from shape analysis should be married with information from other datasets to form a fuller picture of the alpha taxonomy of *H. erectus s.l.*.

To address the aims of this study, a series of comparative analyses of cranial shape among *Homo* species was performed based on different subsets of neurobasicranial landmarks. These subsets were designed to include the maximum number of potential *H. erectus* fossils. Twenty-two fossils assigned to *H. erectus* were studied from Koobi Fora/Ileret, Bouri, Olduvai Gorge, Olorgesailie, Dmanisi, Trinil, Sangiran, Sambungmacan, Ngawi, Ngandong and Zhoukoudian, in addition to representatives of *H. habilis*, *H. rudolfensis*, mid-Pleistocene *Homo s.l.*, *Homo neanderthalensis*, *Homo floresiensis*, and *H. sapiens*.

2. Background

2.1. Is Homo erectus *morphologically distinct?*

A central theme in this debate concerns whether *H. erectus* is morphologically distinct from earlier and later *Homo* species. The issue of sinking *H. erectus* into *H. sapiens* or, conversely, of sinking earlier *Homo* species into *H. erectus* speaks to the fuzzy nature of fossil species boundaries. Additionally, researchers have raised concerns that *H. erectus* is a "grade," morphologically intermediate between *H. habilis* and mid-Pleistocene *Homo*, rather than a "good" species with clear morphological boundaries (Andrews, 1984; Stringer, 1984). Other important questions include how divergent the various subsets of fossils assigned to *H. erectus* are, and what the significance of these differences is. This study will primarily address the first issue (whether *H. erectus* is distinct), but will also provide context relevant for addressing the other two questions.

The older African fossils may not exhibit the full suite of *H. erectus* traits, which blurs the boundary between early *Homo* and *H. erectus*. There is also overlap between the cranial morphologies of traditional *H. erectus* fossils and mid-Pleistocene *Homo* fossils from Europe, Africa and Asia (Wolpoff et al., 1994), and descriptions of fossils currently assigned to *Homo heidelbergensis s.l.* (which itself may consist of multiple species) often emphasized similarities to *H. erectus* (e.g., Ndutu: Clark, 1976; Bodo: Conroy et al., 1978; Omo Kibish II: Day and Stringer, 1982). In addition, the larger and possibly geochronologically younger Ngandong (Solo) fossils have been variably assigned to both *H. erectus* and "archaic *H. sapiens*," suggesting a "fuzzy" boundary between these taxa.

These issues have continued to plague more recent additions to the *H. erectus* hypodigm. The attribution of the ~1.8 Ma (millions of years ago) fossils from Dmanisi, Georgia to *H. erectus* has been challenged on the basis of morphological features shared with *H. habilis* (Rosas and Bermudez De Castro, 1998; Gabunia et al., 2000; Martinón-Torres et al., 2008; Wood, 2011). At the other end

of the spectrum, fossils recently attributed to *H. erectus* from the Dakanihylo ("Daka") member of the Bouri Formation in the Middle Awash of Ethiopia (BOU-VP-2/66) and especially the Dandiero (Buia) Basin in the Danakil Depression of Eritrea (UA-31) present traits seemingly more derived than those seen in *H. erectus* (Antón, 2003). For the Buia cranium (~1.0 Ma), which was provisionally assigned to *H. erectus*, these included vertical lateral cranial walls, a high height: breadth ratio for the neurocranium, no frontal keel, massive supraorbital tori and thinner parietal bones (Abbate et al., 1998; Macchiarelli et al., 2004). The initial description of the ~1.0 Ma Daka cranium emphasizes the resemblance of this fossil to the Buia fossil (Asfaw et al., 2002), and it too has parallel vault walls and other derived features such as an arched temporal squama, double-arched browridges, lack of a transverse occipital torus, and a longer upper than lower scale of the occiput. Similarly, some aspects of the Sambungmacan 3 (Sm 3) cranial morphology, including its more globular neurocranium, steeper frontal bone and less angled occipital, are atypical of classic *H. erectus* morphology and could represent additional taxonomic diversity in Java (Delson et al., 2001; Márquez et al., 2001). There is no definitive geological context for Sm 3, but is suggested to be of Middle Pleistocene age (Kaifu et al., 2006).

Baab (2008a) raised concerns about the attribution by Spoor et al. (2007) of KNM-ER 42700 to *H. erectus*. These concerns were based on the finding that its cranial vault shape fell outside the bounds of variation observed in other *H. erectus* fossils, and intermediate between *H. erectus* and mid-Pleistocene *Homo/H. neanderthalensis*. Spoor et al. (2008) countered that the calvarial shape of KNM-ER 42700 was affected by 1) minor plastic deformation and/or 2) its older subadult or young adult status. Moreover, they expressed concerns about the ability of 3D landmarks to distinguish among *Homo* taxa. The first of these concerns will be addressed here by careful landmark selection and "mirroring" landmarks from the undistorted side. It is also worth noting that a recent analysis confirmed that the shape of the KNM-ER 42700 calvaria falls outside the *H. erectus* range of variation even after a virtual reconstruction removing taphonomic distortion (Bauer and Harvati, 2015). The second concern cannot be addressed entirely in this study, but two other immature *H. erectus* fossils that are likely younger than KNM-ER 42700 will also be examined to see whether a similar set of shape differences characterizes this sample. The power of 3D landmarks to differentiate among *Homo* taxa will also be examined.

Regardless of species definition, there is an expectation that paleontological species can be identified relative to other closely related and potentially morphologically similar species. This distinctiveness need not result from the presence of autapomorphies, but may instead be due to a unique combination of primitive and shared derived features — the combination species definition discussed by Wood (1984). In fact, the loss of primitive features and the addition of more derived features (which may be either unique or shared with later species) through time is plausible if *H. erectus* is a temporally extensive species. Nevertheless, fossils at both ends of the timespan need to hang together on the basis of sufficient shared morphology as to be a cohesive entity. It is therefore valuable to identify if, and in what ways, fossils assigned to *H. erectus* differ from both earlier and later *Homo* species. Various authors have addressed this question in the past based on qualitative descriptions of cranial (and, to a more limited extent, mandibular, dental and postcranial) morphology.

2.2. Defining and diagnosing Homo erectus

The following discussion focuses on the features of traditional *H. erectus* species definitions codified by workers such as Weidenreich (1943), Le Gros Clark (1955), Howell (1978), Rightmire (1990) and Antón (2003), with particular attention paid to the diagnostic value of traits with regard to differentiating *H. erectus* from *H. habilis* and *H. heidelbergensis s.l.*. The emphasis is on features affecting neurobasicranial shape. More localized (discrete) traits often included in *H. erectus* species definitions are summarized in Table 1. There is significant variation in the expression of these features across and even within putative *H. erectus* sites, and many of these traits are primitive for the genus *Homo* or are shared derived characters with later *Homo* species. Very few features, if any, are clearly diagnostic for *H. erectus*, but many may contribute to a combination definition for the species.

The earliest descriptions of *H. erectus* crania were those of Dubois (1894) and Black (1929, 1931). Dubois' (1894) description of the Trinil calotte (type specimen of *Pithecanthrous [Homo] erectus*) focused in large part on comparisons with apes and modern humans, with only a brief reference to the Neanderthal and Spy skulls. He noted several features which remain relevant to defining *H. erectus*: elongated vault that is higher than that of chimpanzees (*Pan*) in lateral view, sharply angled occipital bone with a strongly inclined nuchal plane, a transverse occipital torus, supraorbital tori (superciliary arches) less developed than in *Pan* but more than in the typical *Hylobates*, less post-orbital constriction than in *Pan*, and more extensive development of the nuchal bone inferior to the inferior nuchal line than in

Table 1
Features often cited in *H. erectus* species definitions[a].

Frontal bone
  Sagittal keel
  Coronal keel
  Sagittal and coronal keels contributing to a "4-sided hump" (cruciate eminence)

Parietal bone
  Sagittal keel (often with parasaggital flattening)
  Angular torus

Occipital bone
  Transverse occipital torus
  Vertical separation of inion above endinion
  Occipitomastoid crest
  Lacks a true external occipital protuberance (has only a linear tubercle)

Temporal bone
  Well-developed mastoid and supramastoid crests (sometimes separated by a supramastoid sulcus)
  A wide digastric fossa
  Inwardly-angled tips of the mastoid processes
  Thick tympanic bone
  Less vertically oriented tympanic bone (more prone)
  Thick petrosal crest with a prominent spine
  Petrosal crest terminates medially in a tubercle (processus supratubarius/ infratubarius)
  No styloid process
  No postglenoid process
  Presence of a processus vaginalis variable
  Surface of petrous pyramid smooth
  Long axis of petrosal bone is more antero-posteriorly angled than in humans
  Flat articular tubercle medially
  Entoglenoid formed by the tympanic squama (i.e., no sphenoid spine)
  Fissure between the tympanic plate and the entoglenoid process medially
  Mastoid fissure (between mastoid and tympanic plate)
  Arborized sigmoid sinus

Sphenoid bone
  No infratemporal crest
  Restricted foramen lacerum

Generalized
  Endocranial volume intermediate between apes and humans (both absolutely and relatively)
  Elevated cranial vault thickness

[a] Characters taken from: Dubois (1894), Black (1929, 1931), Weidenreich (1940, 1943, 1950), Santa Luca (1980), Schwartz (2004).

apes. Dubois (1894) also described a bregmatic (or cruciate) eminence (frontal, sagittal and coronal keels that meet at bregma) and a feature that probably corresponds to an angular torus that is continuous with the lateral transverse occipital torus.

Black (1929, 1931) described the first cranial remains of *Sinanthropus pekinensis*, the genus and species name he created for fossils now assigned to *H. erectus* from Zhoukoudian, China. In addition to some of the same features described above, he also noted the flat superior border of the temporal squama, absence of postglenoid and styloid processes, a supraorbital sulcus (described as supraglabellar and more lateral depressions posterior to the supraorbital torus), greatest cranial breadth across the prominent supramastoid crests, laterally diverging vault walls inferior to the parietal tuberosities and convergence of the parietals above the squamosal suture, vertical separation between inion and endinion, and a marked petrosal crest ending medially in a rounded tubercle (probably corresponding to Weidenreich's processus supratubarius/infratubarius; Black, 1931). He also discussed the elevated cranial vault thickness (CVT) of the juvenile Zhoukoudian (Zkd) III (but notes that the bones are thinner in Zkd II). He described the glenoid fossa as deep and antero-posteriorly short but did not find anything about the temporomandibular joint especially distinct from the modern human form. Black (1931) found that Zkd III differed from Kabwe (*H. heidelbergensis*), Neanderthals and modern humans in its particularly low cranial profile and narrow frontal bone based on comparative linear dimensions and indices.

Weidenreich (1940, 1943, 1951) expanded on Black's original description of Zhoukoudian *H. erectus* based on a larger sample, and compared them to fossils of Indonesian *Pithecanthropus*. Weidenreich (1951), as well as Oppenoorth (1932a, 1932b, 1937), also described the Ngandong fossils. Features identified by Weidenreich (1943) arguably formed the core of most subsequent *H. erectus* definitions, which have been refined and expanded by many workers, including: Le Gros Clark (1940, 1955), MacIntosh and Larnach (1972), Jacob (1975), Howell (1978), Howells (1980), Santa Luca (1980), Andrews (1984), Rightmire (1984, 1990, 1998), Stringer (1984), Wood (1984, 1991), Franciscus and Trinkaus (1988), Picq (1990), Wolpoff et al. (1994), Antón (2003), and Kaifu et al. (2008).

The low and elongated vault in norma lateralis may differentiate *H. erectus* from early *Homo*, but conflicting values for the altitudinal index (height/length) complicate this interpretation (Wood, 1984; Tobias, 1991; Lordkipanidze et al., 2006). Maximum cranial breadth is usually across the well-developed supramastoid crests in *H. erectus* (or mastoid processes in some African *H. erectus*), above which the walls converge superiorly. Weidenreich (1943) further describes two inward "bends" in the coronal contour of the mid-vault, one just above the supramastoid crest and one at the parietal tuberosity. Some early *Homo* also exhibit maximum breadth across the mastoid processes but have relatively vertically aligned parietals (Tobias, 1991; Wood, 1991; Villmoare, 2005). Mid-Pleistocene *Homo* fossils often have maximum breadth across the supramastoid crests, but the walls of the vault are more vertical (Bräuer, 2008; Stringer, 2012). Therefore, a well-developed supramastoid crest may have originated during the evolution of *H. erectus*, while the degree of medial convergence of the vault walls could be autapomorphic for the species.

Black (1931) discussed the narrow frontal bone with a supraglabellar depression and more lateral depressions separating the supraorbital torus and the bilateral frontal tuberosities present on Zhoukoudian Skull III. Weidenreich (1943) described this as a single tuberosity spanning between the temporal lines. In either case, the particularly narrow frontal bone and frontal tuberosity are mostly restricted to the Zhoukoudian fossils. The supraorbital sulcus is variably expressed across fossils broadly assigned to *H. erectus*. The supraglabellar depression, for example, is not present in most Indonesian fossils. Moreover, a supraorbital and supraglabellar sulcus have been described for *H. habilis* (e.g., KNM-ER 1813: Wood, 1991) and are present in *H. heidelbergensis* fossils (Asfaw et al., 2008). The generally flat and receding frontal squama is also not clearly diagnostic relative to earlier or later taxa (Stringer, 1984; Rightmire, 1988), and frontal curvature indices based on published values evince substantial overlap among Plio-Pleistocene *Homo* taxa (Lordkipanidze et al., 2006; Kaifu et al., 2008; Rightmire, 2008).

A projecting supraorbital torus is common to all Plio-Pleistocene *Homo* and values for supraorbital thickness overlap between *H. erectus* and later *Homo* (Rightmire, 2008). Nevertheless, shape analyses have recovered differences in the frontal bone generally and supraorbital region in particular between *H. erectus* and mid-Pleistocene *Homo* (Baab, 2007; Athreya, 2009; Freidline et al., 2012). Postorbital constriction was viewed by Wood (1984) as a primitive retention shared with early *Homo*, but was actually reduced in the African and Asian fossils assigned to *H. erectus* relative to the early *Homo* (Lordkipanidze et al., 2006). However, there was overlap among the early *Homo*, putative *H. erectus* (including Dmanisi) and *H. heidelbergensis* ranges (Lordkipanidze et al., 2006; Rightmire, 2008). Several of these features may be influenced by brain size, including relative height of the vault, postorbital constriction and brow ridge development.

The sharply angled occipital bone and longer nuchal than occipital plane differentiate some *H. erectus s.l.* from both earlier and later *Homo*, but at least one mid-Pleistocene *Homo* fossil, Petralona, is also highly angled, and some of the Dmanisi fossils have a more rounded occipital contour (Lordkipanidze et al., 2006; Rightmire, 2008, 2013; Stringer, 2012). The parietal bone has been described as longitudinally flatter and more rectangular (the four borders being more similar in length) in outline than in modern humans but more curved transversely (Weidenreich, 1943). These may be primitive retentions (Andrews, 1984; Stringer, 1984), but published values for the parietal sagittal arcs and chords (used to calculate the parietal sagittal curvature) vary substantially across authors for the same fossils, making it difficult to quantitatively assess sagittal curvature from these values (Tobias, 1991; Lordkipanidze et al., 2006; Kaifu et al., 2008; Rightmire, 2008).

The low, flat and postero-inferiorly sloping superior border of the temporal squama was identified by Andrews (1984) as a primitive retention shared with great apes. However, Terhune and Deane (2008) found that *H. erectus* had a temporal squama that was lower relative to its length than in *Australopithecus afarensis*, *H. habilis* and later *Homo* taxa, but taller than in African apes and similar to *Australopithecus africanus*. Temporal squama shape may therefore be autapomorphic for *H. erectus* within *Homo* (see also Martínez and Arsuaga, 1997), although it is perhaps related to overall vault shape (Terhune and Deane, 2008). The glenoid fossa was described by Black (1931) as deep and antero-posteriorly short but not substantially different from modern humans. Weidenreich (1943), on the other hand, argued that the fossa was deeper relative to its antero-posterior length than in humans or apes.

A more acute petrotympanic angle compared to modern humans has long been part of the *H. erectus* species definition (Weidenreich, 1943, 1951; Howell, 1978). This single angle captures variation in the orientation of the tympanic and petrous elements of the temporal bone. Weidenreich (1943) identified a more sagittally oriented petrous pyramid in Asian *H. erectus* compared to *H. sapiens* (though both were more coronal than in apes). Dean and Wood (1982) confirmed this for African *H. erectus* by showing that they had values at the upper end of the *H. sapiens* range (more sagittally oriented), but nonetheless overlapped both this species and early *Homo* (see also Tobias, 1991). The African *H. erectus* values for tympanic angle also overlapped early *Homo* and *H. sapiens* in this study. Lahr (1996) argued that a less coronally oriented

Table 2
Samples analyzed in this study.

Fossil[1]	Original (O) or Cast (C)	Analysis					
		Trinil	Maximum Fossils	Maximum Landmarks	OH 9	42700	Bodo
H. erectus[2]:							
Trinil	O	X					
S 17	C	X	X	X	X	X	X
S 2	O	X				X	
Zkd 3	C	X	X				X
Zkd 5	C	X	X				X
Zkd 11	C	X	X		X	X	X
Zkd 12	C	X	X		X	X	X
Ng 6	O	X	X	X	X	X	X
Ng 10	O	X		X			X
Ng 11	O	X	X			X	X
Ng 12	O	X	X			X	X
Sm 1	O	X				X	
Sm 3	O	X	X			X	X
Ngawi	C	X					
OH 9	O	X			X		
KNM-ER 3733	O	X	X	X	X	X	X
KNM-ER 3883	O	X	X	X	X	X	X
KNM-WT 15000[2]	O	X				X	
KNM-ER 42700	O	X				X	
D2280	C	X	X	X	X	X	X
D2700	C	X	X	X	X	X	X
D3444	C	X	X	X	X	X	X
Daka	O	X	X	X	X	X	X
KNM-OL 45500[3]	O						
H. habilis							
KNM-ER 1813	O	X	X	X	X	X	X
H. rudolfensis							
KNM-ER 1470	O	X					X
H. neanderthalensis							
La Ferrassie	C	X	X			X	X
La Chapelle	C	X	X		X	X	X
Mid-Pleistocene *Homo*							
Bodo	O						X
Kabwe	O	X	X	X	X	X	X
Omo II	O					X	
Dali	C	X	X	X	X	X	X
Petralona	O	X					X
Ceprano	O		X				X
SH 5	C	X	X	X	X	X	X
Homo floresiensis							
LB1	C					X	
Early *H. sapiens*[4]							
Skhul 5	O		X				
Recent *H. sapiens*[4]							

Andamanese, Afalout-Taforalt, Aboriginal Australian, Austrian, Khoe-San, Chinese, Mongolian, Teita (Kenya), Inuit, Israeli, Anasazi

[1] Abbreviations are as follows: Trnl – Trinil; S - Sangiran; Sm - Sambungmacan; Ng - Ngandong; Zkd - Zhoukoudian; OH - Olduvai Hominid; KNM-ER - Kenya National Museum East Rudolf; KNM-WT - Kenya National Museum West Turkana; D - Dmanisi; KNM-OL - Kenya National Museum Olorgesailie; SH - Sima de los Huesos; LB - Liang Bua
[2] Increasingly inclusive definitions for *H. erectus* are indicated by dashed lines – the most inclusive is the first set of fossils, with each additional set added subsequently.
[3] Analysis of KNM-OL 45500 presented in Supplementary Online Material.
[4] *H. sapiens* only included in expanded maximum fossils analysis

Table 3
Landmarks and definitions.

Landmark	Definition
Inion	Where superior nuchal lines merge in midsagittal plane
Lambda	Apex of the occipital bone at its junction with the parietals, in the midline
Bregma	Posterior border of the frontal bone in the midsagittal plane
Midline post-toral sulcus	Minima of concavity on midline post-toral frontal squama
Glabella	Anterior-most point on frontal bone in Frankfort horizontal
Nasion	Junction of frononasal and internasal sutures
Dacryon	Where lacrimo-maxillary suture meets the frontal bone
Supraorbital notch	Greatest projection of notch into the orbital space, taken on the medial side of the notch
Orbitale	Inferior-most point on margin of orbit
Frontomalare-temporale	Where the fronto-zygomatic suture crosses the temporal line
Frontomalare-orbitale	Where the fronto-zygomatic suture crosses the inner orbital rim
Mid-torus inferior	Inferior margin of superior margin of orbit roughly at the middle of the orbit
Mid-torus superior	Superior aspect of supraorbital torus, directly above mid-torus inferior on anterior aspect of torus
Anterior pterion	Where coronal suture intersects spheno-frontal or spheno-parietal suture
Porion	Uppermost point on the margin of the external auditory meatus
Auriculare	Point vertically above the center of the external auditory meatus at the root of the zygomatic process
Frontotemporale	Where the temporal line reaches its most anteromedial position on the frontal
Parietal notch	Junction of parietomastoid and squamosal sutures
Asterion	Point where the temporal line reaches its most antero-medial position on the frontal
Opisthion	Midline point at the posterior margin of the foramen magnum
Tympanomastoid junction	Where tympanic tube and mastoid fissure meet laterally
Stylomastoid foramen	Posterior border of sylomastoid foramen
Postglenoid process	Infralateral-most point posterior to glenoid fossa and anterior to ectotympanic tube (postglenoid tuberosity or crest)
Inferior entoglenoid	Most inferior point on the entoglenoid pyramid
Lateral articular fossa	Superior-most point on the lateral margin of the articular eminence
Temporo-sphenoid suture	Point where temporo-sphenoid suture passes from squama to cranial base (often on infratemporal crest)
Metopion	Midway between glabella and bregma in midline, calculated a posterieri
Mid-temporal squama	Point midway between glabella and bregma in midline, calculated a posterieri
Mid-parietal	Midway between bregma and lambda in midline, calculated a posterieri

tympanic bone distinguished Ngandong *H. erectus* from *H. sapiens*. In contrast, Martınez and Arsuaga (1997) described *H. erectus* (as well as early *Homo*) as having more coronal tympanic bones compared to their modern human and African (and some of their Eurasian) mid-Pleistocene *Homo* sample. Additional analysis using a single set of measurements and more thorough sampling of fossils is necessary to establish the utility of this trait in delineating among fossil *Homo* species.

3. Material and methods

3.1. Samples

The analyses presented here include fossils usually assigned to the following species: *H. sapiens*, *H. neanderthalensis*, *H. erectus s.l.*, *H. floresiensis*, *H. habilis*, and *H. rudolfensis*. Mid-Pleistocene *Homo* fossils were also examined, which may belong to *H. heidelbergensis s.l.*, or to several species, such as *H. heidelbergensis* and *Homo rhodesiensis* or even the enigmatic "Denisovans." They will be referred to here as mid-Pleistocene *Homo* for simplicity. Original fossils were examined when available and casts when the originals were not accessible, as summarized in Table 2.

The fossils were subjected to several analyses designed to address two questions: (1) Is the calotte/calvarial shape of *H. erectus* distinct from other closely related *Homo* species? (2) How do different fossils attributed to *H. erectus* expand the magnitude and direction of variation in this group? These questions were addressed through interspecific comparisons of increasingly inclusive samples of fossils attributed to *H. erectus*. The most restricted definition of *H. erectus* examined here was that consisting of just the Trinil and Sangiran fossils, because Trinil II is the type specimen of *H. erectus* and the Sangiran fossils are the most comparable in their geography, geochronology and, possibly, morphology (cf. Schwartz, 2004). Subsequently, individual fossils or fossil samples were added based on spatial, geochronological

and historical considerations as indicated by the dashed lines in Table 2. An analysis of the frontal bone performed to investigate the fragmentary Olorgesailie fossil, KNM-OL 45500, is presented in Supplementary Online Material (SOM).

The majority of fossil specimens are adults, with the exception of D2700 from the Eurasian *H. erectus* site of Dmanisi, KNM-ER 42700 from Ileret, KNM-WT 15000 from West Turkana, and possibly Zkd 3. The D2700 subadult fossil has an unfused spheno-occipital synchondrosis and M3s that are erupted but not in occlusion (Vekua et al., 2002; Rightmire et al., 2006). Previous investigations demonstrated that its cranial shape was within the range of other *H. erectus* (Baab and McNulty, 2009) and its neurocranium was within the range of the expected shapes for an adult *H. erectus* of the equivalent size (Baab, 2008b). KNM-ER 42700 was described as a subadult or young adult based on the spheno-occipital synchondrosis being two-thirds fused (Spoor et al., 2007). Age estimates for KNM-WT 15000 range from 7.5 to 15 years of age based on dental and epiphyseal development (as reviewed by Graves et al., 2010). The adult status of Zkd 3 is uncertain (Black, 1929, 1931; Weidenreich, 1943; Mann, 1971; Antón, 2001), but previous geometric morphometric analysis of Asian *H. erectus* indicated that this specimen fits well within the range of cranial morphology exhibited by other Zhoukoudian fossils (Baab, 2010).

3.2. Landmark acquisition and superimposition

Three-dimensional cranial landmarks were acquired using a Microscribe 3D digitizer. The full landmark protocol has been described elsewhere (Baab, 2007), and different subsets of this protocol have been analyzed previously (Baab and McNulty, 2009; Baab, 2010; Baab et al., 2010, 2013). Landmark definitions are in Table 3. Six separate landmark superimpositions were performed by generalized Procrustes analysis (Rohlf and Slice, 1990), one for each of the landmark sets described below.

3.3. Estimation of missing landmarks

Bilateral landmarks missing on one side due to damage or distortion of the original were estimated based on the position of its antimere (if present) using reflected relabeling (Gunz et al., 2009). In a few cases, midline landmarks were estimated based on surrounding morphology or by reference to closely related specimens that preserved a similar morphology in the surrounding (local) region. Details of this approach have been described previously for Kabwe (Broken Hill), Zkd 5, and KNM-ER 1813 (see Baab and McNulty, 2009 for more details), and are described here for the Ceprano and Petralona fossils.

The Ceprano calvaria is a crucial fossil to include in the comparative analyses due to its mix of primitive, *H. erectus*-like features and more derived traits. To do so, the mid-parietal landmark was estimated for Ceprano based on the Zkd 5 morphology because both fossils presented a similar curvature of the remaining portion of the midsagittal suture and the superior median plane of the occipital bone after superimposition. The mid-parietal landmark was positioned midway between bregma and lambda as identified in Ceprano. It is unfortunate that Zkd 5 is the closest anatomical match as this specimen has plaster bridging a gap that begins slightly before bregma and extends to ~50% of the length of the parietal in the median plane. Therefore, the minimum landmark analyses were also re-run without the mid-parietal landmark to assess the effect of including this landmark in the analysis.

To further increase the sample size for mid-Pleistocene *Homo*, the tympanomastoid landmark was estimated for Petralona. Because there was no curve that incorporated this landmark, tympanomastoid was estimated as the average position of this landmark in 22 Plio-Pleistocene *Homo* crania. Using the average position for all *Homo* avoided biasing the analysis in the direction of any particular taxon, but this method of landmark estimation was judged inferior to those approximations discussed above because it was not possible to use the original morphology of Petralona as a guide.

3.4. Corrections for distortion in fossils

A number of the hominin fossils included in the analyses have suffered some degree of postmortem taphonomic deformation. In order to minimize the effects of this distortion, several strategies were employed. For one, landmarks were excluded from regions of localized displacement and reflected from the opposite side if preserved. Examples of this include KNM-ER 1813 where the left supraorbital torus landmarks were reflected from the right side, KNM-WT 15000 where the right lateral supraorbital torus landmarks as well as right parietal notch and asterion were reflected from the left side, and KNM-ER 3883 where the left basicranial landmarks and left porion, parietal notch, and asterion were mirrored from the right side (see Wood [1991] for discussion of distortion in this fossil). Asfaw et al. (2008) document relatively minor distortion in the Daka fossil, most of which was localized rather than systemic. The landmarks most likely to be affected were the right fronto-temporale, fronto-orbitale, and the superior and inferior torus landmarks. No specific corrections were made because this distortion was judged unlikely to affect landmark placement to a great degree.

The mis-alignment of the frontal bone in KNM-ER 42700 (Spoor et al., 2008) appears to have mainly affected the right side and midline of the frontal bone (see also Bauer and Harvati, 2015). Therefore, bilateral frontal bone landmarks (e.g., frontomalare orbitale, frontomalare temporale, frontotemporale, anterior pterion) were reflected from the left while the midline landmarks (glabella, post-toral sulcus) were excluded from analysis. The right side of the cranial base is also offset more anteriorly than the left side, so the postglenoid process, temporosphenoid, and tympanomastoid on the right were also reflected from the left.

3.5. Landmark sets

The first landmark set was restricted to the calotte in order to allow for the inclusion of the type specimen of *H. erectus*, Trinil II

Table 4
Composition of landmark sets.

Landmark	Analysis					
	Trinil	Maximum Fossils	Maximum Landmarks	OH 9	42700	Bodo
Inion	X	X	X	X	X	
Lambda	X	X	X		X	
Bregma	X	X	X		X	X
Midline post-toral sulcus	X	X	X	X		X
Glabella		X	X	X		X
Nasion			X	X		
Dacryon				X		
Supraorbital notch	X	X	X	X		X
Frontomalare-temporale		X	X	X	X	X
Frontomalare-orbitale		X	X	X	X	X
Mid-torus inferior		X	X	X		X
Mid-torus superior		X	X	X		X
Anterior pterion		X	X		X	X
Porion		X	X	X	X	
Auriculare		X	X	X	X	X
Frontotemporale	X	X	X	X	X	X
Parietal notch		X	X	X	X	
Asterion		X	X	X	X	
Opisthion			X	X	X	
Tympanomastoid junction		X	X	X	X	
Stylomastoid foramen			X			
Postglenoid process		X	X	X	X	X
Inferior entoglenoid		X	X	X		X
Lateral articular fossa			X			
Temporo-sphenoid suture		X	X	X	X	
Metopion		X	X			X
Mid-temporal squama		X	X	X		X
Mid-parietal	X	X	X		X	

(Trinil analysis; Table 4) (Dubois, 1894). The first step in this analysis was to assess whether the particular set of landmarks preserved on Trinil II was sufficient to delineate a *H. erectus* calotte shape that is distinct from other *Homo* species, and whether Sangiran fossils share the Trinil morphology (as suggested by Schwartz, 2004). If so, the more complete S 17 and S 2 fossils can be used as proxies for the morphology of the type specimen in subsequent analyses. The Trinil analysis includes a large sample of putative *H. erectus* fossils (Table 2), but the restricted landmark set can provide only limited information about the *H. erectus* cranial morphology. Thus, two additional analyses allow for comparison of overall calvarial shape. The first of these maximizes the fossil sample size while the second maximizes the density of landmark coverage and therefore the amount of morphology captured (termed the maximum fossils analysis and the maximum landmarks analysis, respectively; Tables 2 and 4).

Two landmark sets were designed to include key *H. erectus* or potential *H. erectus* fossils that did not preserve the landmarks in the maximum fossils analysis. One set of landmarks was designed to include the OH 9 fossil (OH 9 analysis; Tables 2 and 4). OH 9 is often viewed as the African fossil with the greatest resemblance to the Asian *H. erectus* sample and was also included by Asfaw et al. (2002) and Gilbert et al. (2008) in the same paleodeme as the Daka fossil for their cladistic analyses. The second was restricted to landmarks present on the KNM-ER 42700 fossil from Kenya (42700 analysis; Tables 2 and 4), which also allowed for the inclusion of KNM-WT 15000. This is a significant addition as both fossils are from Kenya, are subadult individuals, and are of a similar geochronological age (KNM-ER 42700: 1.55 Ma; KNM-WT 15000: 1.51−1.56 Ma) (Brown and McDougall, 1993; Spoor et al., 2007). The final set of landmarks captured the shape of the frontal bone and the lateral aspect of the temporal bone to allow for inclusion of the Bodo fossil (Bodo analysis; Tables 2 and 4). Bodo provides a conservative test of whether *H. erectus* and mid-Pleistocene *Homo* can be distinguished on the basis of cranial shape, as it is one of the oldest mid-Pleistocene *Homo* fossils.

3.6. Statistical analyses

Each set of landmarks was subjected to a standard principal components analysis (PCA), which summarizes the main axes of variation across the entire sample. Both fossils and modern humans were analyzed in the maximum fossils analysis to provide a broad taxonomic context. Only the fossils were analyzed in the other analyses as including *H. sapiens* in the analysis reorients the axes in a way that could mask distinctions among the extinct groups.

A convex hull was drawn around the most restrictive (i.e., exclusive) definition of *H. erectus* − the Trinil and Sangiran fossils − and was then extended to accommodate each addition to the hypodigm as outlined in Table 2. In some instances, the fossils added were within the distribution of previously included fossils. In this case, the convex hull was not extended. A shaded convex hull was also used to delineate the mid-Pleistocene *Homo* sample. Principal component (PC) scores were regressed on the natural logarithm of endocranial volume (EV) when axes reflected taxonomic variation to explore whether the aspects of shape separating groups could be attributed to simple scaling effects or whether a species deviated from a common size-shape trajectory. This represents a difference from the more common practice of regression scores on the logarithm of centroid size. Endocranial volume was used because cranial superstructures and cranial vault thickness affect the centroid size values. However, the natural logarithm of centroid size was used rather than EV for the analysis that included modern humans, as EVs were not available for the recent human sample.

Although PC axes are statistical constructs that are not a priori biologically meaningful, it is probable that the most variable aspects of morphology in an interspecific sample of primarily adult specimens will align with taxonomic differences. However, between-group principal components analyses (BG-PCA), which emphasize differences among groups rather than among individuals, were also performed. In a BG-PCA, only the group averages are used to calculate PCs, and the full sample is then projected onto these components (axes; Mitteroecker and Bookstein, 2011). Between group-PCA was chosen in preference to canonical variates analysis as this is more appropriate for analyses involving small samples and large numbers of variables (Mitteroecker and Bookstein, 2011). Two BG-PCAs were performed for the 42700 and Bodo landmark sets which contained a good balance between sample sizes, landmark coverage and focal fossils. One BG-PCA was based on five a priori groups: early *Homo* (*H. habilis* and *H. rudolfensis*), Neanderthals, mid-Pleistocene *Homo*, African/Georgian *H. erectus* and Asian *H. erectus* (see Table 1). The second BG-PCA was the same, except the two early *Homo* species were separated (only relevant to the Bodo analysis) and fossils assigned to *H. erectus* were divided into the following temporo-geographic groups: early Indonesian, late Indonesian, Chinese, African, and Georgian. Daka and KNM-ER 42700 were not categorized a priori in either of these analyses and were not included in the calculation of the axes.

Daka and KNM-ER 42700 were not assigned to a group a priori because results from the standard PCAs demonstrated significant morphological differences between these two fossils and the other African fossils assigned to *H. erectus*. Results were summarized by an unweighted pair-group average (UPGMA) cluster analysis of Euclidean distances based on the four non-zero eigenvectors that completely described differences among the five groups.

Using the same two landmark sets, the pairwise Procrustes distances among fossils assigned to *H. erectus*, mid-Pleistocene *Homo*, and *H. neanderthalensis* were calculated. The range of interspecific values based on distances among fossils assigned to these three species (but not within each group) was presented. Then, different subsets of intraspecific distances were calculated: distances within the mid-Pleistocene *Homo* group (including the distance between the two Neanderthal fossils), distances among all fossils assigned to *H. erectus* (with the exception of KNM-ER 42700 and Daka), distances among just the Asian fossils assigned to *H. erectus* and distances among just the African/Georgian fossils assigned to *H. erectus*. Distances of the Daka fossil to fossils assigned to *H. erectus* from Africa and Georgia, to fossils assigned to *H. erectus* from Asia and to mid-Pleistocene *Homo* were also presented. Finally, distances from KNM-ER 42700 to the African/Georgian fossils assigned to *H. erectus* were computed.

4. Results

4.1. Trinil landmark set: PCA

Part of the *H. erectus* hypodigm was distinct from other *Homo* species based on the restricted anatomical regions preserved in the *H. erectus* type specimen (Trinil II). The Asian fossils assigned to *H. erectus*, as well as KNM-ER 3733 and KNM-ER 3883 were differentiated from mid-Pleistocene *Homo*, early *Homo* (*H. habilis* and *H. rudolfensis*) and *H. neanderthalensis* on PCs 1 and 4 combined (Fig. 1). The Trinil and Sangiran fossils occupied a central position within the Asian *H. erectus* scatter while the Zhoukoudian and Turkana Basin fossils were isolated at the positive end of PC 1. The younger Indonesian and some Dmanisi fossils (D2700 and D3444) extended the range in the opposite direction (the negative end of PC 1). The former scored high on PC 4, thus separating them
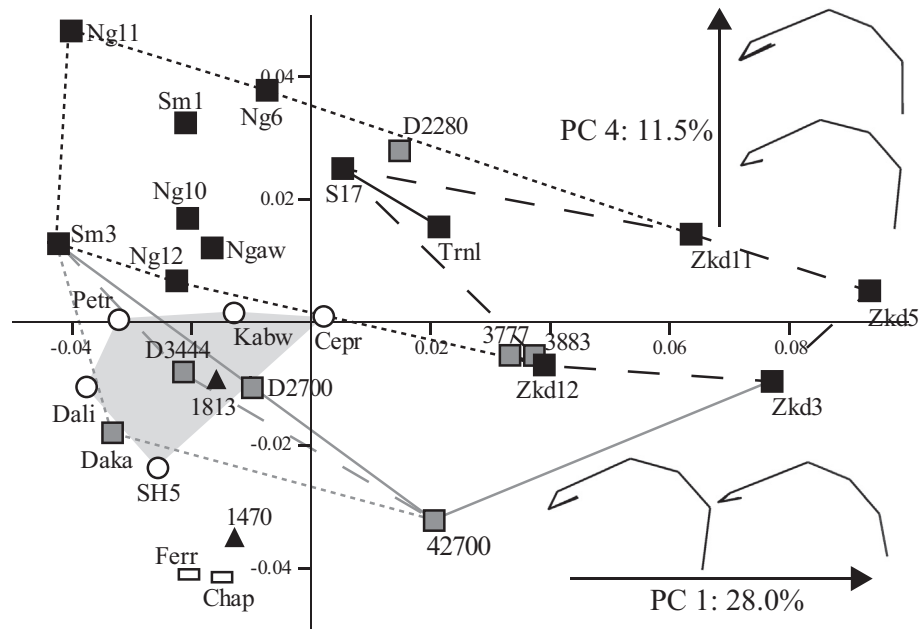
Figure 1. Principal components ordination based on Trinil landmark set. Principal components 1 and 4, which showed the best distinction between *H. erectus* and other fossil taxa, are shown. Symbols are as follows, black squares: fossils assigned to Asian *H. erectus*; gray squares: fossils assigned to African and Georgian *H. erectus*; circles: mid-Pleistocene *Homo*; triangle: early *Homo*; rectangle: *H. neanderthalensis*. Convex polygons circumscribe increasingly inclusive definitions of *H. erectus* as follows, solid black: Trinil and Sangiran fossils; large black dashes: + Zhoukoudian fossils; small black dashes: + Ngandong, Sambungmacan and Ngawi fossils; solid gray: + African fossils; large gray dashes: + Dmanisi fossils; small gray dashes: + Daka fossil (see Table 2). The solid gray convex hull surrounds mid-Pleistocene *Homo*. Wireframes connecting landmarks are used to show shape change from the negative to the positive extremes of the axes in left lateral view.

from other species, while the latter scored lower on PC 4 and thus overlapped the distribution of mid-Pleistocene *Homo* and *H. habilis*. The Dmanisi fossils were distinct from these species on PC 2. Daka was positioned close to the mid-Pleistocene *Homo*/ *H. habilis* cluster on PCs 1, 2 and 4. KNM-ER 42700 scored lower than all *H. erectus* fossils on PC 4 and was not associated with any of the taxonomic clusters in the subspace spanned by PCs 1 and 4. Size did not account for a significant proportion of the variance on PC 1 or 4.

The second PC strongly contrasts KNM-ER 42700 , and, to a lesser extent, D3444, from the remainder of the sample (SOM Fig. 1). All fossils assigned to *H. erectus* were distinct from *H. habilis*/ *H. rudolfensis* on PC 3 except D2280 (Dmanisi) (SOM Fig. 1). KNM-ER 3733 and D3444 also plotted close to early *Homo* on this component. Size accounted for 19% ($p = 0.02$) and 32% ($p < 0.01$) of variance in PC 2 and 3 scores, respectively. The scaling relationship on PC 2 is strongly influenced by the low score of the small KNM-ER 42700 fossil; the significant relationship between PC 2 score and size disappears when it is excluded from the regression. This suggests that shape differences between KNM-ER 42700 and other *Homo* species do not follow size-shape trends seen in the genus *Homo* generally.

4.2. Maximum fossils landmark set: PCA

Landmarks included in this analysis captured overall cranial vault shape, with the exception of the nuchal plane of the occipital bone. When extinct *Homo* taxa were analyzed alongside recent *H. sapiens*, there was an archaic-to-derived trajectory of cranial shape variation along a combination of PCs 1 and 2 wherein the sole representative of *H. habilis*, KNM-ER 1813, was contrasted with modern humans. *H. erectus,* mid-Pleistocene *Homo* and Neanderthals were arrayed between them, with *H. erectus* positioned closest to *H. habilis* (Fig. 2). The direction of maximal interspecific

differentiation was roughly orthogonal to the direction of maximal intraspecific variation for all groups except Neanderthals, which were, however, represented by only two specimens.

Daka consistently clustered with the mid-Pleistocene *Homo* and *H. neanderthalensis* groups; Sm 3 approached this distribution but did not overlap it. The two Neanderthals scored slightly lower than any other fossils except KNM-ER 1813 (*H. habilis*) on PC 3 (not figured). PC 4 can also be viewed as an archaic-to-derived trajectory, but only within the fossil taxa. In this context, the shape of the D3444 vault was more similar to Asian *H. erectus* than other Dmanisi fossils and Sm 3 and Daka overlapped the mid-Pleistocene *Homo*/Neanderthal distributions.

Regressions of the first and third components on the logarithm of centroid size were statistically significant, but the amount of variance explained by size on PC 3 was trivial ($R^2 = 0.04$, $p < 0.01$). The relationship on PC 1 ($R^2 = 0.11$, $p < 0.01$) was also weak, and modern humans consistently scored higher than fossil hominins even when centroid sizes overlapped.

Excluding the *H. sapiens* sample resulted in clearer distinction among the extinct groups. *H. habilis* and most fossils attributed to *H. erectus* were separated from the more derived *Homo* taxa on PC 1, although the later Indonesian *H. erectus* sample approached the mid-Pleistocene *Homo* range (Fig. 3). In contrast, the sole *H. habilis* fossil, KNM-ER 1813, was very distinct from the remainder of the archaic *Homo* sample on the second component. The Afro-Georgian portion of the *H. erectus* sample was positioned closer to *H. habilis* than was the Asian portion, with most later Indonesian and Zhoukoudian fossils being equidistant from *H. habilis*. The third component separated the late Indonesian from the Zhoukoudian and Turkana Basin fossils, while PC 4 distinguished the mid-Pleistocene *Homo* sample from Neanderthals (SOM Fig. 2). All Dmanisi fossils scored low on PC 4.

The somewhat extreme position of the Zkd 5 cranium on PC 2 could be affected by its reconstruction, as the large frontal bone
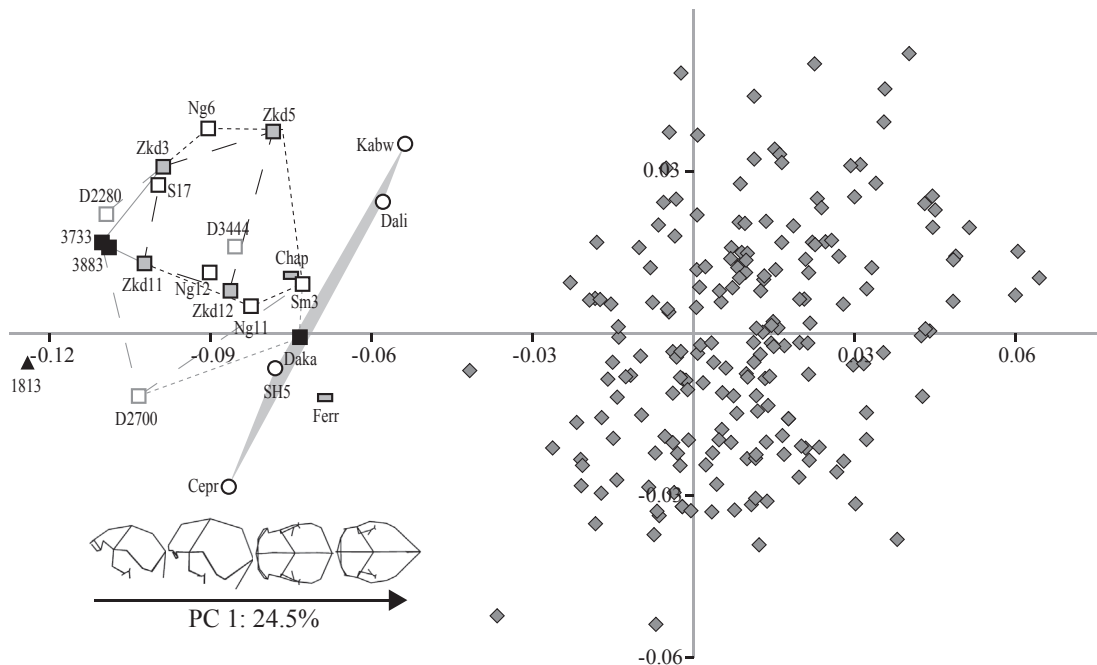
Figure 2. Principal components ordination based on maximum fossils landmark set of fossils and recent *H. sapiens*. Principal components 1 and 4, which showed the best distinction between *H. erectus* and other fossil taxa, are shown. Legend same as Figure 1, with the addition of diamonds: *H. sapiens*. Wireframes connecting landmarks are used to show shape change from the negative to the positive extremes of PC 1 in left lateral and superior views.

fragment does not directly articulate with the posterior neuro-cranium (the two pieces were discovered during separate excavations in the 1930s and 1960s [Weidenreich, 1943; Qiu et al., 1973]). For example, a rotation of the two elements to create a slightly greater height and less receding frontal squama might bring its shape closer to the remainder of the *H. erectus* sample. However, other elements of shape captured by PC 2, such as the wider mid-vault relative to the temporomandibular joint or the greater antero-posterior distance between asterion and inion, are unlikely to be affected by the reconstruction.

Twenty eight per cent of variance in PC 1 scores ($p = 0.01$), which distinguished between most fossils assigned to *H. erectus* (except Daka) and later *Homo* taxa, was accounted for by differences in EV. At the same EV, *H. erectus* consistently scored higher than Neanderthals and particularly mid-Pleistocene *Homo*. This pattern was most marked for the Zhoukoudian *H. erectus* and least apparent for D3444 and Sm 3. Daka behaved like the more derived *Homo* fossils rather than *H. erectus*. The second component, which separated *H. habilis* from other *Homo* fossils, also reflected allometric variation ($R^2 = 0.39$, $p < 0.01$). Superficially, this suggests that some of the differences in shape between *H. habilis* and *H. erectus* are related to the larger size of the latter. However, KNM-ER 1813 (*H. habilis*) scored much higher than predicted for its size. The two Neanderthals and SH 5 (Sima de los Huesos) to a lesser extent also score higher on PC 2 than predicted by their brain size. Therefore, a common allometric scaling effect cannot explain the shape differences between *H. erectus* and other *Homo* taxa.

As discussed in Materials and methods above, the analysis was re-run without the mid-parietal landmark since its estimation in Ceprano may be problematic. The same basic patterns emerged, with *H. habilis* scoring very high on PC 2, in particular contrast to Zkd 5, and *H. erectus* differed from later *Homo* species along PC 1. The most notable difference was the higher scores on PC 2 for most mid-Pleistocene *Homo*/Neanderthal/Daka fossils, with the exception of Ceprano. One result of this shift was to bring the Dali and Kabwe fossils closer to Ceprano.

4.3. Maximum landmarks landmark set: PCA

The maximum landmarks analysis included an additional three bilateral and two midline landmarks which more completely captured frontal, temporal and occipital morphology. The primary axis of variation differentiated early *Homo* from mid-Pleistocene *Homo* and Neanderthals, with most fossils assigned to *H. erectus* occupying an intermediate position between these two extremes but closer to the latter (Fig. 4A). A large proportion of the variance in scores along the first axis was attributable to size differences ($R^2 = 75\%$; $p < 0.01$) (Fig. 4B). While the mid-Pleistocene *Homo* fossils scored higher than similarly-sized *H. erectus*, this difference was negligible for SH 5 (European mid-Pleistocene *Homo*). Daka and D3444 had larger positive residuals, while KNM-ER 1813 and 3733 had larger negative residuals, indicating that not all early *H. erectus* fossils are characterized by a similar scaling relationship. A regression line based on only fossils assigned to *H. erectus* (with the exception of Daka) further highlights that both earlier and later *Homo* species differ from the allometric trajectory within this group.

The sole Sangiran fossil (S 17) occupied an intermediate position along PCs 1 and 2 among fossils assigned to *H. erectus* (and therefore lower on PC 2 than the other species). The other Asian fossils extended the *H. erectus* range toward mid-Pleistocene *Homo* on PC 1 and even further away from the rest of the *Homo* sample on PC 2. Most African and Georgian fossils extended the range toward *H. habilis*, but D3444 extended the *H. erectus* range much higher on PC 2. Daka was positioned very close to the mid-Pleistocene *Homo* range on PCs 1 and 2. Size accounted for less than 10% of shape differences on PC 2, but showed a clear distinction between large *H. erectus* and mid-Pleistocene *Homo* (as well as Daka). D3444 also scored higher than predicted for its brain size. The third component (13.2%) further distinguished KNM-ER 1813 from other *Homo* fossils and separated the single Neanderthal fossil (La Chapelle-aux-Saints) from the mid-Pleistocene *Homo* sample. Both of these fossils were most strongly contrasted on this axis from the Dmanisi fossils and S 17. The relationship with size was not statistically significant.
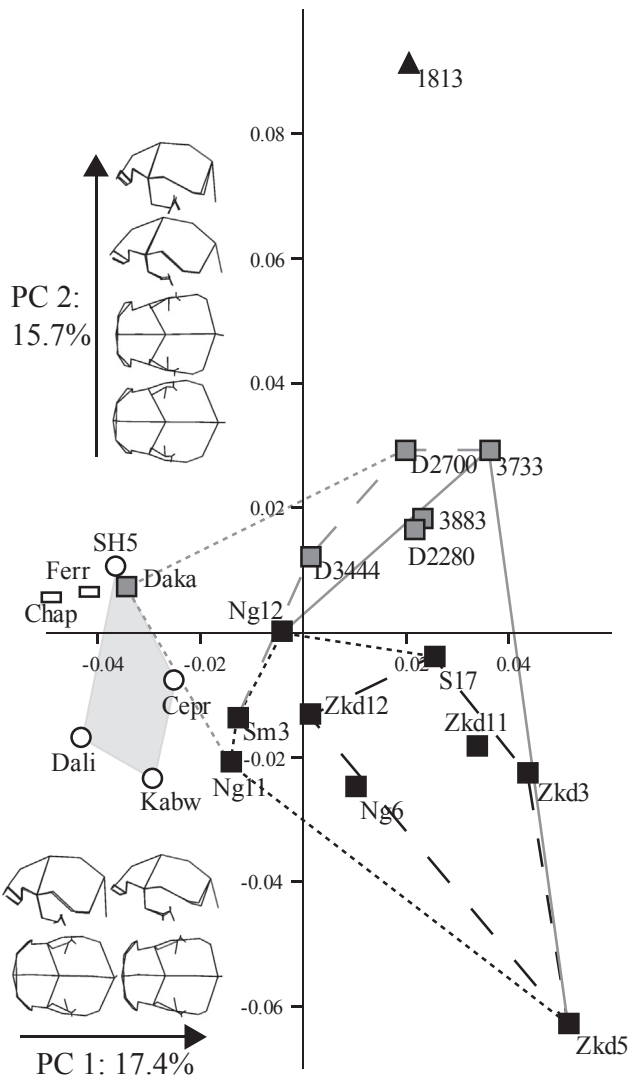
Figure 3. Principal components ordination based on maximum fossils landmark set of fossils only. Principal components 1 and 2, which showed the best distinction between *H. erectus* and other fossil taxa, are shown. Legend same as Figure 1. Wireframes connecting landmarks are used to show shape change from the negative to the positive extremes of the axes in left lateral and superior views.

4.4. OH 9 landmark set: PCA

The ordination along the first two PCs of the OH 9 landmarks bore resemblances to that of the maximum landmarks analysis discussed above despite the absence of midline landmarks from the superior vault. The primary axis of variation contrasts KNM-ER 1813 (*H. habilis*) and mid-Pleistocene *Homo*/Neanderthals, with most fossils assigned to *H. erectus* positioned between these extremes but closer to the latter (Fig. 5). Again, S 17 was positioned centrally within the scatter of potential *H. erectus* fossils. Other Asian fossils scored low on PC 2 and some scored closer to more derived *Homo* on PC 1. African and Georgian fossils were positioned between S 17 and *H. habilis*. OH 9 (as well as KNM-ER 3883 and D2280) clustered near to S 17 while KNM-ER 3733 and the other Dmanisi fossils scored higher on PC 2. Daka was positioned close to mid-Pleistocene *Homo* on PCs 1 and 2. OH 9 had the highest score on PC 3, but was again closest to other African *H. erectus* (not shown). Variation along PC 1 was related to overall size ($R^2 = 0.70$; $p < 0.01$). The regression analysis was very comparable to that

reported for the previous analysis (Fig. 4B), with OH 9 plotting very close to S 17.

4.5. 42700 landmark set: PCA

Principal components 1 and 3 together provided the greatest separation among the taxonomic clusters (Fig. 6) and the first component again contrasted *H. habilis* and mid-Pleistocene *Homo*/*H. neanderthalensis,* with most *H. erectus* arrayed between these endpoints. The two Sangiran fossils were not as centrally positioned on PC 1 as in the maximum landmarks or OH 9 analyses due to their higher scores. The Zhoukoudian and particularly the younger Indonesian fossils extended the putative *H. erectus* range toward later *Homo* on PC 1 and away from other *Homo* fossils on PC 3. The African and Georgian fossils scored higher on the third component than the Asian fossils with the exception of Zkd 12. D3444 and KNM-WT 15000 overlapped Asian *H. erectus* on the first component, while KNM-ER 3733, KNM-ER 3883, D2280 and D2700 extended the range toward *H. habilis* on this component. Daka overlapped the mid-Pleistocene *Homo* range on PCs 1–3. KNM-ER 42700 plotted close to mid-Pleistocene *Homo* in the subspace spanned by PCs 1 and 3, but exhibited fairly extreme scores on PCs 2, 3 and 4 (especially PC 2). KNM-WT 15000 generally occupied a more central position, but was at the opposite extreme to KNM-ER 42700 on PC 2 (not figured). This is significant as both of these fossils are approximately the same geochronological age and both are immature individuals. Omo 2 overlapped the edge of the Asian *H. erectus* range. Size accounted for 47% ($p < 0.01$) of the variance in PC 1 scores, but there was substantial dispersion around the regression line. In general, fossils assigned to *H. erectus* had higher scores than mid-Pleistocene *Homo* when their EVs overlapped in size. However, D3444, Daka, Sm 3 and, particularly, KNM-ER 42700 had lower scores.

As discussed above, some of the frontal bone landmarks were excluded from this analysis due to plastic deformation of the frontal bone. While frontomalare temporale, frontomalare orbitale and frontotemporale were recorded only from the left side, where distortion appeared minimal (and mirrored to the right side), it remains possible that these landmarks were still affected by the plastic deformation that affected the rest of this region. Thus, the PCA was re-run without these three landmarks. The *Homo* species were fairly well separated in the subspace of PCs 1 and 2. Although KNM-ER 42700 overlapped both *H. erectus* and mid-Pleistocene *Homo* on PC 1, it was isolated by its uniquely high score on PC 2, in contrast to LB1 (*H. floresiensis*; SOM Fig. 3). The two *H. neanderthalensis* crania were also more distinct on the first component because the relatively high and wide vault of La Chapelle-aux-Saints was emphasized by this particular set of landmarks.

4.6. Bodo landmark set: PCA

The Bodo analysis included landmarks from the frontal and temporal bones that addressed the shape of these bones as well as their position and orientation relative to one another. Overall, the Bodo analysis resembled the maximum fossils analysis already presented, in that the first axis separated the *H. erectus* samples and later *Homo,* while early *Homo* (in this case *H. habilis* and *H. rudolfensis*) were distinguished along the second axis. Daka overlapped the mid-Pleistocene *Homo* range on both axes. It differed, however, in that the two Neanderthals were inserted between *H. erectus* and mid-Pleistocene *Homo* on PC 1. S 17 occupied an intermediate position along PC 2 but had a higher position on PC 1 than many putative *H. erectus* fossils. Most African and Georgian fossils extended the range toward early *Homo* on PC 2. The Chinese
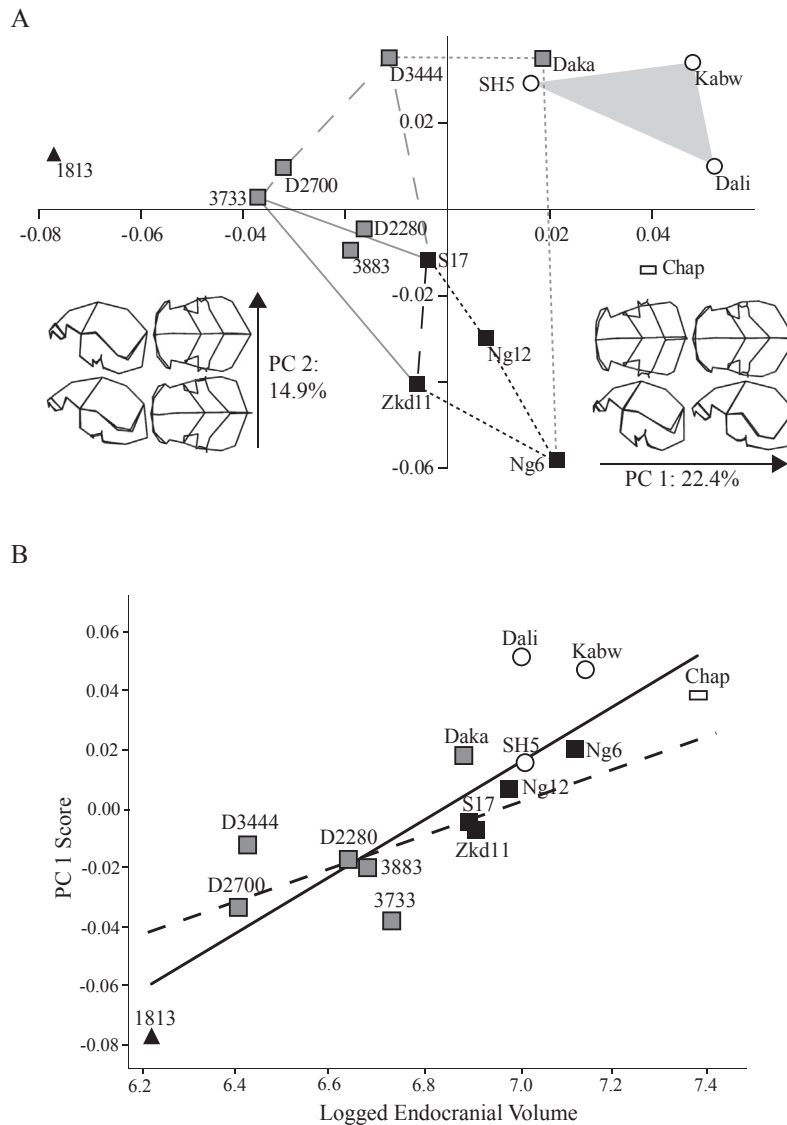
Figure 4. Principal components ordination based on maximum landmarks landmark set (A) and regression of PC1 scores on logged endocranial volume (B). Principal components 1 and 2, which showed the best distinction between *H. erectus* and other fossil taxa, are shown. Legend same as Figure 1. Wireframes connecting landmarks are used to show shape change from the negative to the positive extremes of the axes in left lateral and superior views. The solid regression line is based on the entire sample whereas the dotted regression line was based on only those fossils assigned to *H. erectus* with the exception of Daka.

H. erectus were strongly contrasted with later *Homo* while Ngandong/Sambungmacan were more clearly contrasted with early *Homo*. The latter group did not approach mid-Pleistocene *Homo*/Neanderthals, as they did in other analyses.

Size had a moderate influence on the position of fossils along both axes (PC 1: $R^2 = 0.17$; $p = 0.04$; PC 2: $R^2 = 0.34$; $p < 0.01$). On the first axis, mid-Pleistocene *Homo* and Daka scored well above the regression line (and therefore higher than comparably sized *H. erectus*) while most Zhoukoudian fossils and Ng 6 scored lower than predicted by this scaling relationship. Indonesian *H. erectus* and Dali scored higher-than-predicted for their size on PC 2 while early *Homo*, Bodo and Neanderthals scored particularly low for their size. In other words, groups occupying the extremes of PC 1 or PC 2 had large residuals from the size-shape regression line for that axis.

4.7. UPGMA clustering

As a way of examining between group variation, three sets of UPGMA trees were generated for the 42700 landmark set, which

captured mid- and posterior vault morphology and the Bodo landmark set, which captured frontal and temporal bone morphology. The three sets of trees were based on: 1) scores from the standard PCA (i.e., individual variation), 2) scores from a BG-PCA based on eight (42700 landmark set) or nine (Bodo landmark set) a priori groups, and 3) scores from a BG-PCA based on five a priori groups. In the second case, the trees reflect variation among taxa as it relates to the shape differences among the a priori identified groups.

The distances among individuals and clusters increased as more groups (or single individuals) were the basis of analysis, and fossils were more likely to cluster in the "wrong" taxon in the analysis of individuals. *H. erectus* formed a single cluster in the five-group PCA (Fig. 8 a,d) but was split into two clusters in the other analyses. The late Indonesian *H. erectus* fossils formed a cluster that was more similar to late *Homo* than other *H. erectus* based on the 42700 landmarks (Fig. 8 b,c), perhaps related to allometric trends. All Indonesian and Georgian fossils assigned to *H. erectus* form a cluster that was more similar to later *Homo* taxa when the Bodo
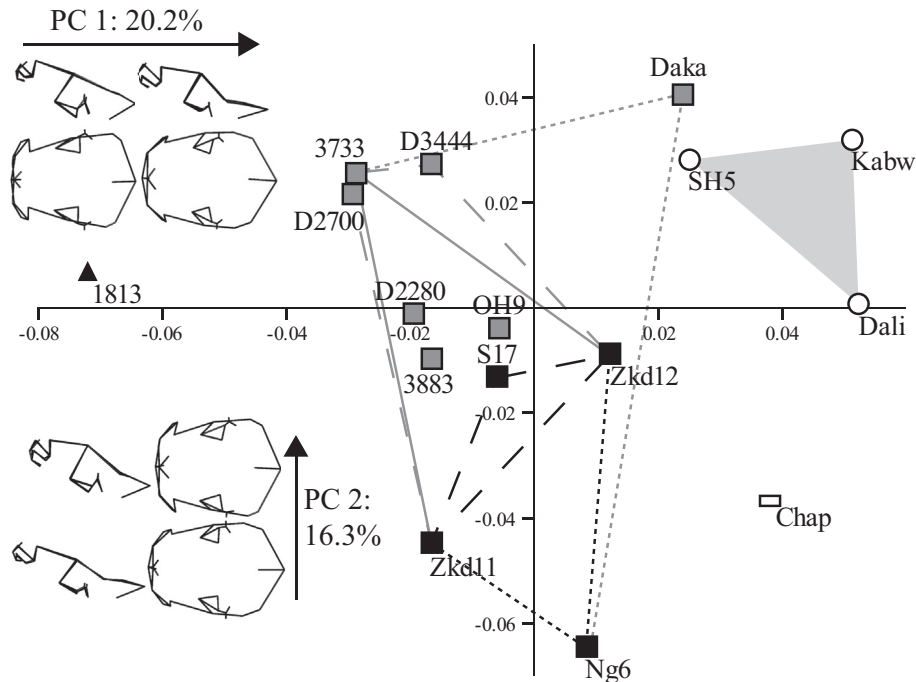
Figure 5. Principal components ordination based on OH 9 landmark set. Principal components 1 and 2, which showed the best distinction between *H. erectus* and other fossil taxa, are shown. Legend same as Figure 1. Wireframes connecting landmarks are used to show shape change from the negative to the positive extremes of the axes in left lateral and superior views.

landmarks were used (Fig. 8 e,f), a pattern unlikely to be related to size. Mid-Pleistocene *Homo* and the Daka fossil were in the same cluster, linked to a Neanderthal cluster, in most analyses (Fig. 8). KNM-ER 42700 also clustered with the former group in the trees based on the BG-PCAs but was on its own branch in the tree based on individuals (Fig. 8 a–c). Many of the temporogeographic clusters within *H. erectus s.l.* (i.e., paleodemes) were consistently recovered, including the later Indonesian fossils, the Georgian fossils and KNM-ER 3733/3883. Interestingly, S 17 grouped with the Georgian

Figure 6. Principal components ordination based on 42700 landmark set. Principal components 1 and 3, which showed the best distinction between *H. erectus* and other fossil taxa, are shown. Legend same as Figure 1, with the addition of the inverted triangle: *H. floresiensis*. Wireframes connecting landmarks are used to show shape change from the negative to the positive extremes of the axes in left lateral and superior views.

fossils and S2 with the Zhoukoudian fossils in all analyses except the 5-group BG-PCA (Fig. 8 b,c, e,f), thus confirming their morphologically intermediate position within the larger *H. erectus s.l.* sample. The major division among fossils assigned to *H. erectus* in the 42700 trees was broadly along size-lines, with the exceptions of Daka, Sm 3, and KNM-WT 15000 that clustered with the larger Indonesian fossils.

4.8. Magnitude of shape distances

The patterns of pairwise Procrustes distances based on the 42700 and Bodo landmark sets were similar. The median interspecific Procrustes distance was higher than any of the median intraspecific values (Fig. 9). The median intraspecific *H. erectus* value was higher than the median intraspecific value calculated for the later *Homo* species, which was likely driven by the higher within African/Georgian and between Asian and African/Georgian distances, as the within Asian distances were lower. There was, however, extensive overlap in the ranges of inter- and intraspecific distances.

It is apparent that KNM-ER 42700, despite being from the same geographic region and general time period as the African fossils assigned to *H. erectus*, and despite the inclusion of the KNM-WT 15000 juvenile in the sample, is very distinct from this group. The distances of Daka to members of mid-Pleistocene *Homo* were very low, lower than from Daka to fossils assigned to *H. erectus*. The median distance of Daka to African/Georgian *H. erectus* was higher than the distance to Asian fossils based on the 42700 landmarks, but the pattern was reversed using the Bodo landmarks. This latter result is probably due to the more extreme positions of the Zhoukoudian fossils on PC1 and the Ngandong/Sambungmacan fossils on PC 2 in the Bodo PCA. This difference presumably related to differences in landmark composition as the 42700 landmark set was missing many landmarks from the frontal bone while the Bodo analysis was primarily frontal bone landmarks.
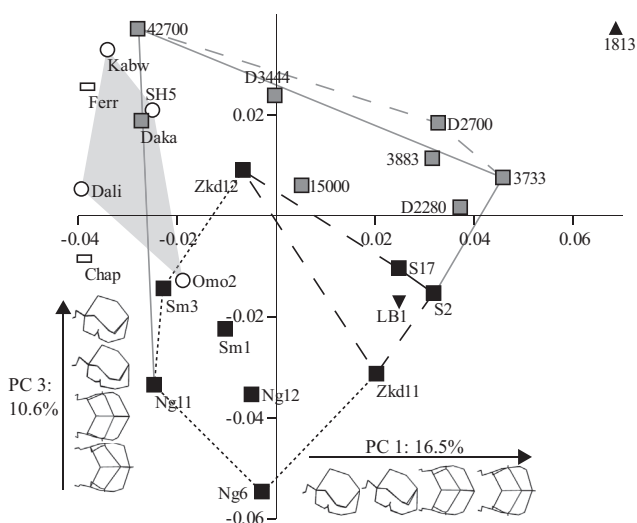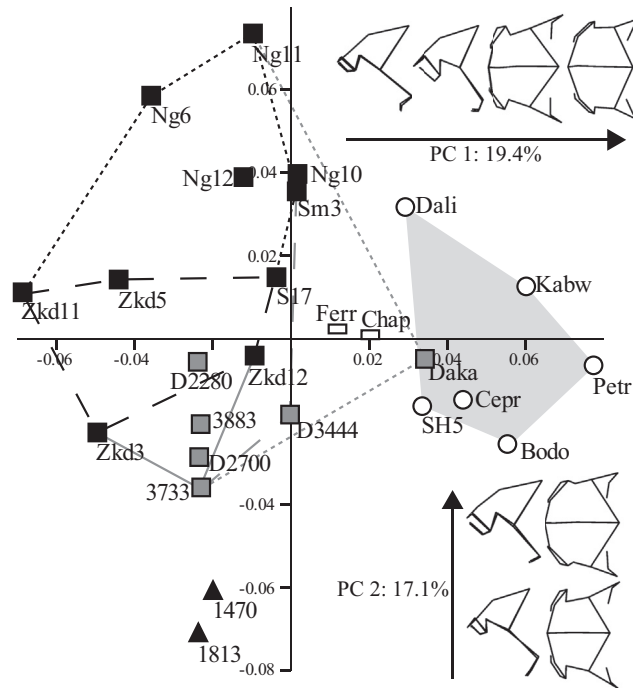
Figure 7. Principal components ordination based on Bodo landmark set. Principal components 1 and 2, which showed the best distinction between *H. erectus* and other fossil taxa, are shown. Legend same as Figure 1. Wireframes connecting landmarks are used to show shape change from the negative to the positive extremes of the axes in left lateral and superior views.

5. Discussion

5.1. Distinctiveness of H. erectus cranial shape

A major goal of this study was to assess the distinctiveness of *H. erectus* on the basis of neurocranial shape. *H. erectus* differed from modern humans due to the more globular shape of the human cranial vault with a relatively long and vaulted parietal bone, more vertical frontal squama, diminutive supraorbital torus, minimal constriction behind the orbits, high temporal squama, narrower occipital bone, antero-inferiorly angled occipital plane, wide mid-vault, and narrow cranial base. This characterization of the human neurocranium accords well with previous descriptions (Day and Stringer, 1982; Lieberman et al., 2002; Bruner et al., 2003; Trinkaus, 2006; Mounier et al., 2011), but did not capture features such as parietal bossing.

The *H. erectus s.l.* sample examined here was also consistently and widely separated from early *Homo* on the basis of its relatively antero-posteriorly longer and vertically shorter cranial vault, long and flat frontal bone, greater posterior projection of inion, less inferiorly projecting entoglenoid process and greater breadth of the neurocranium compared to both the supraorbital torus and the cranial base. Very few studies have addressed the distinction between the cranial vault of early *Homo* and *H. erectus*, although Wood (1991) noted the evolution of a longer cranium in *H. erectus* (and *H. sapiens*) relative to early *Homo*. Other features that separate the two taxa include localized traits such as an angular torus or a prominent petrotympanic crest with a process supratubarious, and aspects of the facial skeleton (e.g., broader nasal bones and a more convex lateral malar; Turner and Chamberlain, 1989; Rightmire, 1990; Antón, 2004) not captured by the landmarks used here.

The distinction between fossils assigned to *H. erectus* and later *Homo*, particularly mid-Pleistocene *Homo*, was also apparent, but the ranges of the two groups more closely approached each other

and there was some overlap among these groups in the individual PCAs and UPGMA clustering based on individual variation. However, the separation between these groups was clearer when the frontal bone was considered (e.g., the maximum landmarks and Bodo analyses). In all cases, the 1.0–0.8 Ma Daka fossil grouped with mid-Pleistocene *Homo*. Moreover, some of the overlap was due to Omo 2, a fossil assigned here to mid-Pleistocene *Homo* (Bräuer, 2008; Rightmire, 2008) but whose taxonomic affinities are uncertain. McDougall et al. (2005) assigned Omo 2 to early *H. sapiens* based on their inference that it derived from the same stratigraphic level as the more modern-looking Omo 1 fossil, and was therefore dated to ~195 ka (thousands of years ago). Omo 2 was, however, a surface find and its archaic morphology has been documented in several studies (Friess, 2003; Rightmire, 2008; Gunz et al., 2009). The interpretation of this result is uncertain given its unknown geological age and the fact that Omo 2 was only complete enough to include in one analysis. This result could indicate morphological overlap between species, the presence of "an archaic, late-surviving lineage, present alongside anatomically modern humans" (Rightmire, 2008: 12), or that this landmark set was insufficient to distinguish among taxa.

H. erectus (with the exception of Daka) differed from mid-Pleistocene *Homo* in its more postero-inferiorly angled (i.e., less vertical) and shorter occipital plane, less superiorly expanded vault, more inferiorly projecting entoglenoid process, longer and lower temporal squama, greater postorbital constriction and relatively narrower vault at mid-temporal squama. The supraorbital torus was also flatter across its superior margin, narrower medio-laterally and thinner (supero-inferiorly) at mid-torus. Consistent with these observations, characterizations of mid-Pleistocene *Homo* frequently include references to its high, arched temporal squama, laterally expanded and more vertical parietals, a less angled occipital and strong supraorbital tori (e.g., Rightmire, 2007; Bräuer, 2008; Stringer, 2012). However, there is considerable variation in the expression of these features and overlap between *H. erectus* and mid-Pleistocene *Homo* in individual traits (Rightmire, 2008; Mbua and Bräuer, 2012). For example, Rightmire (2008) observed a number of traits that differed between *H. erectus* and mid-Pleistocene *Homo*, but the ranges of the two taxa often overlapped (e.g., relative brain size, postorbital narrowing, occipital proportions and angulation and possibly cranial base flexion). The analyses presented here indicate that overall neurocranial shape distinguishes between *H. erectus* and mid-Pleistocene *Homo* even if individual measurements overlap, and this was particularly apparent in the frontal bone. Compared to Neanderthals, the vault was lower and the supraorbital torus was straighter (less arched over each orbit). The *H. erectus* vault was also wider posteriorly but more constricted posterior to the orbits.

5.2. Scaling

Differentiation of fossils assigned to *H. erectus* and to later *Homo* taxa occurred on PC 1 and was always correlated with endocranial volume. This relationship was especially strong ($R^2 \geq 0.70$) when early *Homo* was also differentiated from putative *H. erectus* along this axis (in a direction opposite to later *Homo*). Even when early *H. erectus* was distinguished from early *Homo* and later *Homo* on orthogonal axes, endocranial volume accounted for a significant proportion of variation on both axes. In both cases, most *H. erectus* (with the exception of D3444) had residuals from the regression line in the opposite direction to mid-Pleistocene *Homo*. Increased endocranial volume was related to features including a decrease in postorbital constriction, a more robust supraorbital torus, a relatively wider mid-vault, and a more inferiorly positioned posterior temporal squama (parietal notch). Therefore, the shape variation

UPGMA trees based on PCA of individuals (no a priori groups)
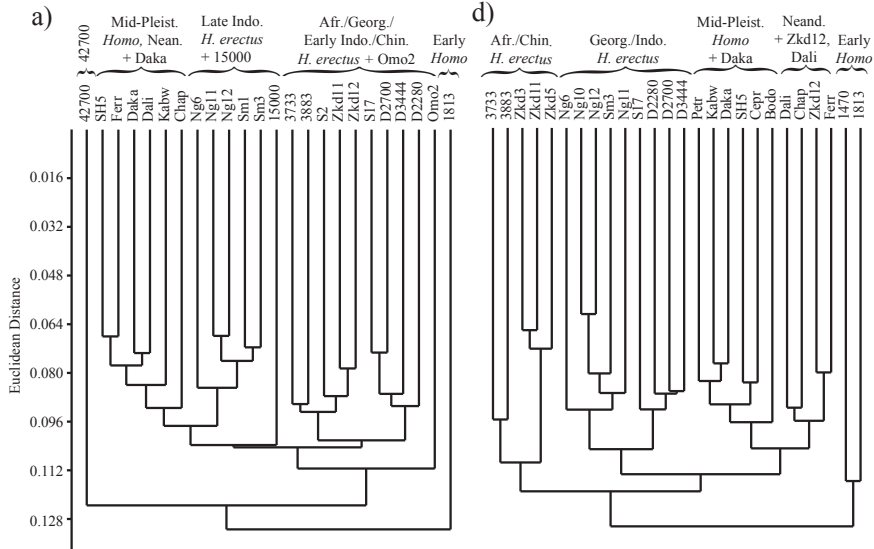
UPGMA trees based on BG-PCA with 8-9 a priori groups
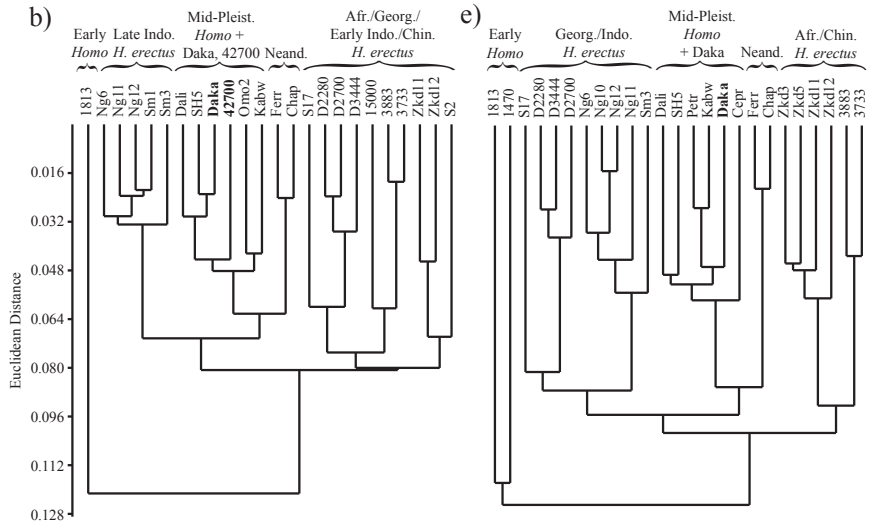
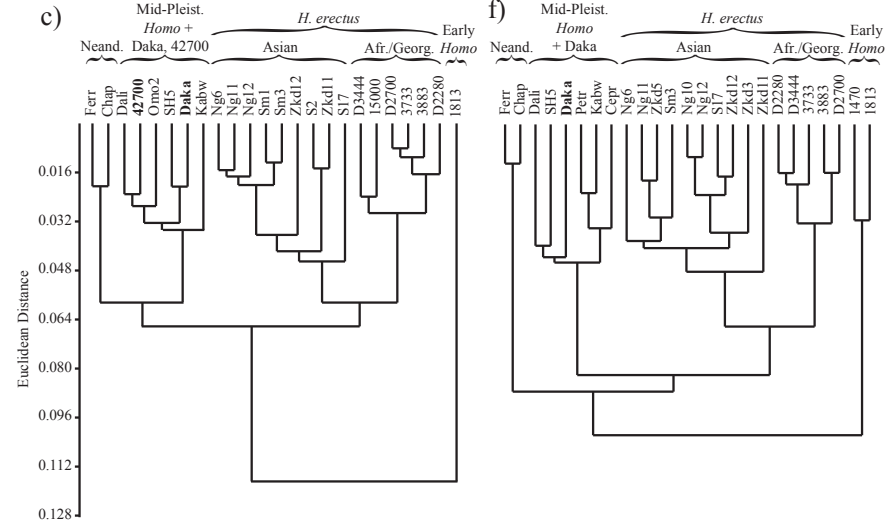**UPGMA trees based on BG-PCA with 5 a priori groups**

Figure 8. UPGMA trees based on scores from standard PCA of individuals (a, d), a BG-PCA with numerous a priori groups (b, e) and a BG-PCA of a small number of a priori groups (c, f). The trees in the left column (a, b, c) are based the 42700 landmark set while the right column (d, e, f) are based on the Bodo landmarks.
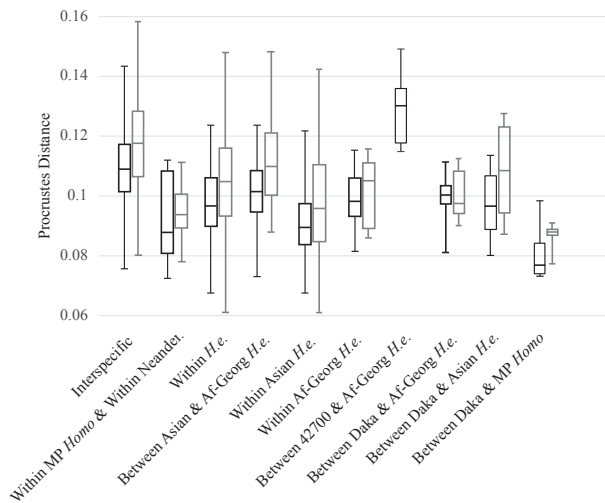
Figure 9. Box-and-whisker plots of Procrustes distances. Distances were calculated using the 42700 landmark set (black outlines) and the Bodo landmark set (gray outlines). Medians, first and third quartiles and the minimum and maximum values are presented. *H. erectus* is abbreviated *H.e.*

among taxa and within the *H. erectus* sample was correlated with differences in endocranial volume, but differently signed residuals from the regression line in *H. erectus* and mid-Pleistocene *Homo* indicated that changes in endocranial volume are insufficient to explain all shape differences between these groups. In other words, brain size increases in the *H. erectus* sample led to different cranial shape evolution than did brain size increases in mid-Pleistocene *Homo*.

5.3. Spatiotemporal variation in the H. erectus sample

Regional and chronological variation in the *H. erectus* sample was apparent in several analyses, but the analysis of Procrustes distances confirmed that intraspecific differences were of a lesser magnitude than interspecific ones. To some extent, intraspecific variation is better assessed in an analysis restricted to *H. erectus* fossils, as the PC axes here are influenced by interspecific variation. What is of interest in this study is how different temporo-geographically circumscribed populations assigned to *H. erectus* relate to one another in the context of interspecific variation.

The Sangiran fossils are a useful starting point for thinking about alpha taxonomy of *H. erectus* because they were similar to Trinil II (the less complete type specimen), positioned close to the center of the distribution of the fossils assigned to *H. erectus*, and consistently differed from the other *Homo* taxa (see also Schwartz, 2004). Adding the Zhoukoudian fossils to this most conservative definition of *H. erectus* generally expanded the direction of shape variability away from other *Homo* fossils. The late Indonesian fossils (e.g., Ngandong and Sambungmacan) further increased shape variation in the group, usually in the direction of later *Homo* along PC 1 but further from all other fossils along PC 2. The greater affinity of later Indonesian fossils and mid-Pleistocene *Homo* along PC 1 is due in part to the larger size of both groups of fossils despite some shape divergence between the two groups at overlapping sizes. Portions of the Asian *H. erectus* hypodigm, either from later Indonesian sites or from Zhoukoudian, were often isolated along either PC 1 or 2, confirming previous analyses that have highlighted distinctions among the Asian paleodemes (Antón, 2002; Kidder and Durband, 2004; Kaifu et al., 2008; Zeitoun et al., 2010). The shape differences that distinguished these populations were not clearly related to variation in endocranial volume and may instead result from genetic drift

caused by geographic isolation and/or local adaptation of the spatially widespread *H. erectus* populations (Antón, 2002).

Included in the later Indonesian fossils were Ngawi and Sm 3, both more recent additions to the hypodigm. The Ngawi fossil fell comfortably within the *H. erectus* range of variation and showed affinities to other *H. erectus* fossils from Ngandong and Sambungmacan, in line with previous descriptions and analyses of the Ngawi fossil (Sartono, 1991; Widianto et al., 2001; Widianto and Zeitoun, 2003; Durband, 2006). Sm 3 generally fell at the edge of the *H. erectus* distribution in the direction of the mid-Pleistocene *Homo* sample due to its more globular neurocranium, but was more closely aligned with *H. erectus* in frontal bone shape (Fig. 7; SOM Fig. 4). Sm 3 was very distinct from *H. sapiens* in its 3D calvarial shape in the present study despite having a (2D) midsagittal profile intermediate between fossil *Homo* and *H. sapiens* (Delson et al., 2001) and a median frontal squama profile like that of recent humans (Bruner et al., 2013). Importantly, it was always near the Ngandong, Sm 1 and Ngawi fossils in morphospace (see also Antón et al., 2002), and likewise shares many discrete traits with these groups (Delson et al., 2001; Antón et al., 2002). There is thus no compelling evidence from this study to exclude any of these fossils from a species that includes Sangiran/Trinil.

The addition of KNM-ER 3733, 3883 and OH 9 extended the shape variation toward early *Homo* and away from both of the later *Homo* species as well as the Zhoukoudian and later Indonesian fossils assigned to *H. erectus*. This basic pattern is consistent with previous work that has emphasized the more primitive and generalized nature of early African *H. erectus* and the more distinct and derived morphology of Asian *H. erectus*, and is also an expected result if early African *H. erectus* is near the stem of the species. The closer resemblance of KNM-ER 3733 and 3883 to early *Homo* was also due in part to their small size. The larger OH 9 fossil was more similar to S 17, which was similar in size and possibly geochronological age (Larick et al., 2001; but see; Hyodo et al., 2011) despite its geographic distance. KNM-WT 15000 grouped with *H. erectus* but had a higher vault and less projecting occipital bone than other Turkana Basin *H. erectus*, presumably related to its immature status. Importantly, the Sangiran/Trinil fossils bridged the gap between older but more geographically distant fossils from Africa and more geographically proximate but geochronologically younger fossils from Asia. The other African fossils considered here (Daka and KNM-ER 42700) defy the basic patterns just described and are discussed subsequently.

Of the three Georgian fossils considered, D2280 and D2700 generally fell in or near the range of variation of the *H. erectus* sample, and overlapped the Koobi Fora fossils on the first few components. Despite favorable comparisons with early *Homo* (Gabounia et al., 2002; de Lumley et al., 2006), these fossils were more similar in overall vault shape to the Koobi Fora *H. erectus*, and on higher components often grouped with Indonesian *H. erectus* (e.g., PC 3 in SOM Fig. 2). Of the three Dmanisi fossils, D2700 was the most similar to early *Homo*, but was morphologically closer to *H. erectus* than early *Homo*. Therefore, although they introduce additional variation, they behaved as expected for small and geochronologically older members of the species positioned between Africa and Asia. Similarities to both African and Asian (particularly Sangiran) *H. erectus* have been noted elsewhere with regard to both the crania and mandibles from Dmanisi (Bräuer and Schultz, 1996; Rosas and Bermudez De Castro, 1998; Rightmire et al., 2006).

D3444 showed more affinities with mid-Pleistocene *Homo* than did the other African/Georgian fossils. This was a result of a more vertical occipital plane, less posteriorly projecting inion (due in part to its low transverse occipital torus) and a more robust supraorbital torus. Despite these similarities, D3444 clustered with *H. erectus*,

and specifically with other Georgian fossils, and retained primitive features lost in more derived *Homo*, including a low squamosal suture, inferiorly projecting entoglenoid process, a narrower mid-vault, marked postorbital constriction, sagittal keeling on the parietals, and a reduced foramen lacerum (Lordkipanidze et al., 2006). When the frontal bone and the mid- and posterior vault were evaluated separately (SOM Figs. 3 and 4), D3444 was more clearly associated with *H. erectus*, suggesting it is the shorter and higher vault that drives its convergence on the mid-Pleistocene vault shape. Thus, both D3444 and Sm 3 approached the condition of mid-Pleistocene *Homo* more closely than their geographic contemporaries, but they did so in different ways. In common with later *Homo*, both had relatively short and tall vaults, but D3444 also had a more robust supraorbital torus and proportionately shorter frontal bone (antero-posteriorly), whereas Sm 3 had greater breadth across the mid-vault and less constriction across frontotemporale.

Taken as a whole and in conjunction with evidence from discrete traits, the Dmanisi sample should probably be included in *H. erectus*, with the recognition that these fossils expand variation in *H. erectus*, and not always in the direction of early *Homo*. Some features of D3444 would then be interpreted as individual variations that superficially converge on the mid-Pleistocene *Homo* condition. In fact, some of these features are likely related − the proportionately shorter frontal bone and less projecting inion together result in a shorter vault, which, when scaled to the same size as other *H. erectus*, appears relatively tall. Given that D3444 and the newly described D4500 are the most robust of the five Dmanisi crania and quite different in shape from one another, it is unlikely that either pattern can be entirely attributed to sexual variation.

This study was not designed to address the question of multiple species, but some of the results are nevertheless relevant to this question. The results described above accord with descriptions of *H. erectus* as a species that shared a "total morphological pattern" (sensu Le Gros Clark, 1959) distinct from other species, with intraspecific variation in qualitative and metric traits across its range (e.g., Weidenreich, 1951; Rightmire, 1990; Antón, 2003; Kaifu et al., 2008). The fact that median distance among fossils assigned to *H. ergaster* (excluding KNM-ER 42700 and Daka) was lower than the median interspecific distance is compatible with a single species model. Previous studies have shown that the magnitude of shape variation in *H. erectus* is within the bounds of some single neontological species despite its greater time depth, but exceeds others (Kramer, 1993; Villmoore, 2005; Baab, 2008b), particularly in the temporal bone (Terhune et al., 2007). Perhaps more important is the fact that the Trinil/Sangiran fossils were equally distant from other Asian fossils as early African ones sometimes assigned to *H. ergaster*. The relationship among paleodemes of *H. erectus* corresponded with geographic, temporal and allometric differences, common sources of intraspecific variation. For example, the early and late Indonesian fossils differed from early African/Georgian fossils in the same direction. The greater distance of the latter can be explained by their larger size and/or longer genetic isolation.

This interpretation is not without some problems. UPGMA clusters based on individual variation failed to uncover a single *H. erectus* clade, indicating very real variation within this sample. Interestingly, the UPGMA analysis highlighted different patterns of geographic clustering based on the mid- and posterior vault versus the frontal and temporal regions. This could reflect a complex pattern of population history or mosaic evolution of the vault. In neither case were the divisions among populations along traditional *H. ergaster* − *H. erectus sensu stricto* (*s.s.*) lines. The 42700 landmark set was more heavily weighted toward the posterior cranium, including the occipital bone, which is a less reliable

indicator of modern human population history than several other cranial bones (von Cramon-Taubadel, 2009). The Bodo landmark set included information from only the frontal and temporal bones, both good indicators of human population history, and possibly hominin phylogeny more generally (von Cramon-Taubadel, 2009). Therefore, the Bodo landmark set may be a better indicator of population history. In this context, different evolutionary scenarios may be invoked to explain the Indonesian/Georgian and the African/Zhoukoudian clusters including ancestor−descendant relationships and gene flow, but homoplasy cannot be ruled out. More explicit population genetic models may help to discern between these scenarios.

Although the median within-group distance for *H. erectus* was less than the interspecific distance, the ranges overlapped substantially (Terhune et al., 2007), and it was higher than the intraspecific distance for later *Homo* species. *H. erectus* also occupied a greater region of morphospace than the equally geographically diverse mid-Pleistocene *Homo* sample, possibly due to its greater time depth or stronger population structure or, alternatively, because it contains more than one species. Finally, neurocranial shape is only one aspect of anatomy that needs to be considered. For example, the vault shape of LB 1 overlapped *H. erectus* but its mandible and dentition differ in meaningful ways from this species (e.g., Brown and Maeda, 2009).

Therefore, although the early African/Georgian fossils differed only subtly from later Asian ones in their vault shape, these results do not specifically refute the two species solution. If *H. ergaster* is recognized because discrete traits indicate it is ancestral to later *Homo* whereas Asian populations were an evolutionary "dead end" (e.g, Wood, 1984), then the Georgian sample could be assigned to *H. ergaster* based on the extensive overlap in neurocranial shape. Cranial vault shape did not support the idea that some African fossils represent *H. ergaster* and others *H. erectus s.s.* (e.g., OH 9 [Wood, 1994]) nor that Daka bridged the two species and thus blurred this particular species boundary (Asfaw et al., 2002).

5.4. Consideration of problematic fossils

Two African fossils, Daka and KNM-ER 42700, are more problematic as members of *H. erectus*, even broadly defined, and thus deserve more careful consideration. Including Daka in *H. erectus* not only expands the range of variation encompassed by *H. erectus*, but effectively erases the boundary between *H. erectus* and later *Homo* species such as *H. heidelbergensis s.l.* or *H. rhodesiensis* in Africa. Daka exhibited a tall cranial vault relative to cranial length, a proportionally shorter frontal bone with wide, tall and arched supraorbital tori, a less posteriorly projecting inion, and proportionally greater breadth at mid-vault and frontotemporale relative to the posterior vault. Rightmire (2013) recently performed an analysis aimed at assessing patterns of covariation within the cranium and their relationships to endocranial volume and ectocranial dimensions in *H. erectus* (including Daka) and mid-Pleistocene *Homo*. Although difficult to compare directly to the results presented here, it appears that while Daka conformed to the *H. erectus* condition in most aspects, it differed from *H. erectus* in its relatively tall cranial vault above porion (relative to cranial length and breadth) and its thick supraorbital torus (relative to overall cranial size), in agreement with some of the results presented here.

Asfaw et al. (2002) used a cladistic analysis of 22 characters to evaluate the position of a paleodeme (sensu Howell, 1999) that consisted of Daka, OH 9, and the Buia cranium from Eritrea. The result of the latter analysis (and several other variants presented in Gilbert et al. [2008]) did not support separate African and Asian *H. erectus* clusters. Together, these results led Asfaw et al. (2002: 317) to argue that "the 'Daka' calvaria's metric and morphological

attributes centre it firmly within *H. erectus*. Daka's resemblance to Asian counterparts indicates that the early African and Eurasian fossil hominids represent demes of a widespread palaeospecies." While it is true that the cladistic analyses did not support a division between *H. erectus s.s.* and *H. ergaster*, these analyses also did not support a separation between *H. erectus s.l.* and fossils attributed to more derived *Homo* species and therefore cannot be read as unambiguously supporting the assignment of Daka to *H. erectus*. The use of paleodemes may also mask important variation among individuals (Manzi et al., 2003), and the analysis may have been strongly influenced by the inclusion of endocranial volume (Antón, 2003). Clustering based on phenetic distances derived from presence/absence data for 22 *H. erectus* and mid-Pleistocene *Homo* fossils grouped Daka with the East Turkana *H. erectus*, but also indicated that Daka was distinct from the typical *H. erectus* pattern in the direction of mid-Pleistocene *Homo* (Manzi et al., 2003). However, the assessment of character states for some fossils was problematic (e.g., postorbital constriction [Gilbert et al., 2003]).

Although the Daka calvaria undoubtedly shares anatomical features with *H. erectus*, a number of these are also retained in some members of mid-Pleistocene *Homo*, including midline keeling of the frontal bone, an angular torus and greatest width in the supramastoid/mastoid region (Rightmire, 1996, 2008; Mbua and Bräuer, 2012). Moreover, some traits seen in Daka, such as more vertical parietal walls with parietal bossing, a vertical occipital plane, a longer upper than lower scale of the occiput, a sphenoid spine, and a high arched temporal squama (Asfaw et al., 2008; Gilbert et al., 2008), are typically considered derived for mid-Pleistocene *Homo* relative to *H. erectus* (Rightmire, 1996, 2007, 2008; Terhune and Deane, 2008; Rightmire, 2009; Stringer, 2012). Although Asfaw et al. (2008) compared the arched condition of the supraorbital tori in Daka to that seen in KNM-ER 3733, the tori of the latter is much less vertically expanded and the superior margin is flatter. The tori of Daka more closely resembles the condition in certain mid-Pleistocene *Homo*, including Kabwe, Saldanha, Ceprano, Bodo, and Petralona. The presence of derived features in an African fossil that may pre-date the documented time range of *H. heidelbergensis* or *H. rhodesiensis* by as little as 200 thousand years (Bodo is ~0.6 Ma and Daka was found in deposits 1.0−0.8 Ma) is perhaps not entirely surprising. Yet, analyses of discrete features have come to conflicting conclusions regarding the phylogenetic position of Daka − Mounier et al. (2011) found that Daka fell within the *H. erectus s.l.* clade and was most similar to OH 9 and KNM-ER 3883 based on distances calculated from discrete traits while Argue (2015) argued that Daka grouped with mid-Pleistocene *Homo*, particularly Bodo and Ceprano, based on cladistic analysis of cranial traits.

The relatively small endocranial volume of 992−995 cm³ for the Daka calvaria (Asfaw et al., 2002; Gilbert et al., 2008) is lower than those recorded for mid-Pleistocene *Homo*, which range from 1100 to 1430 cm³ (Rightmire, 2013). However, the Salé fossil from Morocco, also proposed to be an early member of mid-Pleistocene *Homo* (Hublin, 1985, 2001), has a comparably small endocranial volume of 930−960 (Jaeger, 1975) or 880 cm³ (Holloway, 1981). The analyses presented here include most well-preserved *H. erectus* fossils, including fossils with endocranial volumes that overlap the mid-Pleistocene *Homo* range, yet the Daka calvaria is the only focal fossil to consistently group with mid-Pleistocene *Homo*. A value of ~995 cm³ is plausible if Daka belonged to an early population of *H. heidelbergensis s.l.* or *H. rhodesiensis* that was descended from African *H. erectus*, whose documented endocranial volumes range from ~727 to 1067 cm³ (Holloway, 1975, 1978).

The overlapping calvarial shape shared between Daka and members of mid-Pleistocene *Homo* can be interpreted as an example of individual variation that converged on the mid-

Pleistocene *Homo* pattern in a population otherwise more similar to *H. erectus*. Although convergences in cranial shape do occur, the presence of both a more derived cranial shape and cranial non-metric traits suggests that the resemblance of Daka to mid-Pleistocene *Homo* reflects evolutionary change in that direction rather than convergence. Most likely, Daka was a member of an "advanced" population of *H. erectus* that was ancestral to a later *Homo* species (e.g., *H. heidelbergensis* or *H. rhodesiensis*) and whose cranial shape strongly foreshadowed that group or an early member of a later *Homo* species that includes individuals like Bodo and Kabwe that were studied here, as well as Saldanha and Ndutu that were too incomplete to include.

KNM-ER 42700, the 1.5 Ma fossil from Kenya, did not cluster with other small early Pleistocene fossils from Africa or Georgia. Instead, this fossil often occupied a distinct region of shape space that did not overlap with other hominin taxa (Fig. 6 and SOM Fig. 1), and was more likely to converge on the more derived *Homo* species rather than early *Homo* due to its higher cranial vault with reduced constriction behind the supraorbital tori. Issues of distortion in the landmark set were minimized in this analysis, but still confirmed an earlier analysis that did not adjust for distortion in the fossil (Baab, 2008a), as well as an analysis that corrected for deformation by performing a virtual reconstruction of the calvaria (Bauer and Harvati, 2015). Therefore, deformation is unlikely to explain the position of this fossil outside of the range of *H. erectus* calvarial shape.

It remains possible, however, that the seemingly unusual morphology of KNM-ER 42700 is attributable to its immature status. Two other juvenile/subadult fossils assigned to *H. erectus*, D2700 and KNM-WT 15000, did not behave similarly to KNM-ER 42700 in this analysis. D2700 generally clustered with other Georgian fossils. KNM-WT 15000 appeared more similar to Asian *H. erectus* than did other African fossils from the Turkana Basin on PC 1 (Fig. 6), and was particularly similar in its position to D3444. The more rounded vault of KNM-WT 15000 was likely due in part to its particularly young age (~8 years of age based on enamel histology [Dean et al., 2001]) and minimally developed cranial superstructures. The spheno-occipital synchondrosis of KNM-ER 42700 is 2/3 fused and it was originally described as a young adult or late subadult (Spoor et al., 2007). Based on this evidence, KNM-ER 42700 was older than D2700 (whose synchondrosis was less fused), which was itself likely older than KNM-WT 15000 based on M3 eruption (Rightmire et al., 2006). The immature status of KNM-ER 42700 is an unlikely explanation for the distinctiveness of its calvarial shape compared to other small early Pleistocene *H. erectus* unless the spheno-occipital synchondrosis is a poor indicator of age. Additional research regarding ontogenetic shape change in *H. erectus* and the true developmental age of the KNM-ER 42700 fossil could further clarify this issue.

The original description of KNM-ER 42700 included a multivariate analysis of linear dimensions and a comparison of discrete features among Plio-Pleistocene *Homo* and this fossil. Specific traits listed in support of its *H. erectus* attribution were keeling on the frontal and parietal bones, a medio-laterally narrow mandibular fossa, coronally oriented tympanic and sagittally oriented petrous parts of the temporal bone, a short occipital scale, and close approximation of opisthocranion and lambda. As discussed previously, additional work is necessary to establish the utility of either the petrous or tympanic angles in differentiating among fossil *Homo* taxa. More problematic is the fact that early African and Georgian fossils assigned to *H. erectus* have previously been described as having a "glenoid fossa … wide mediolaterally" (Antón, 2003, p. 137) and opisthocranion is nearly coincident with inion (not lambda) in *H. erectus* (e.g., Weidenreich, 1943; Wood, 1984). Therefore, only two (midline keeling and short occipital

scale) or perhaps three (orientation of the petrous and tympanic) of the listed characters support the initial attribution of KNM-ER 42700 to *H. erectus*. Assuming that KNM-ER 42700 is truly an older subadult or young adult, then its calvarial shape argues against its inclusion in *H. erectus*. Combined with the ambiguous discrete character evidence, it remains "… preferable to assign KNM-ER 42700 to *Homo* sp. in order to emphasize the uniqueness of this fossil's morphological pattern" (Baab, 2008a: 745).

6. Conclusions

H. erectus retained a characteristic cranial form for a period of over one million years and across a geographic range that extended from East Africa to Eurasia and the Far East. This study has demonstrated that this cranial shape is in part intermediate between earlier *Homo* species and more derived species such as *H. heidelbergensis* or *H. rhodesiensis* but is in part also unique, particularly in the Asian members of the species. Recent additions to the species from Sambungmacan, Ngawi, and Dmanisi expanded the range of variation but generally showed the greatest affinities to other *H. erectus* fossils that were geographically and temporally proximate. Additions to *H. erectus* from Africa did not show particular affinities to *H. erectus*. The Daka fossil more closely resembles mid-Pleistocene *Homo* in overall vault form, and also exhibits a number of more derived discrete traits with this species, while KNM-ER 42700 remains a morphological outlier relative to the Plio-Pleistocene *Homo* fossils analyzed here.

Acknowledgements

Supplementary Online Material

Supplementary online material related to this article can be found at http://dx.doi.org/10.1016/j.jhevol.2015.11.004.

References

Abbate, E., Albianelli, A., Azzaroli, A., Benvenuti, M., Tesfamariam, B., Bruni, P., Cipriani, N., Clarke, R.J., Ficcarelli, G., Macchiarelli, R., Napoleone, G., Papini, M., Rook, L., Sagri, M., Tecle, T.M., Torre, D., Villa, I., 1998. A one-million-year-old *Homo* cranium from the Danakil (Afar) Depression of Eritrea. Nature 393, 458–460.

Andrews, P., 1984. An alternative interpretation of the characters used to define *Homo erectus*. Cour. Foursch. Senck. 69, 167–175.

Antón, S.C., 2001. Cranial growth in *Homo erectus*. In: Minugh-Purvis, N., McNamara, K.J. (Eds.), Human Evolution Through Developmental Change. Johns Hopkins University Press, Baltimore, pp. 349–380.

Antón, S.C., 2002. Evolutionary significance of cranial variation in Asian *Homo erectus*. Am. J. Phys. Anthropol. 118, 801–828.

Antón, S.C., 2003. Natural history of *Homo erectus*. Yearb. Phys. Anthropol. 46, 126–170.

Antón, S.C., 2004. The face of Olduvai Hominid 12. J. Hum. Evol. 46, 335–345.

Antón, S.C., Márquez, S., Mowbray, K., 2002. Sambungmacan 3 and cranial variation in Asian *Homo erectus*. J. Hum. Evol. 43, 555–562.

Argue, D., 2015. Variation in the Early and Middle Pleistocene: The phylogenetic relationships of Ceprano, Bodo, Daka, Kabwe and Buia. In: Behie, A.M., Oxenham, M.F. (Eds.), Taxonomic Tapestries: The Threads of Evolutionary, Behavioural and Conservation Research. ANU Press, Canberra, pp. 215–248.

Asfaw, B., Gilbert, W.H., Beyene, Y., Hart, W.K., Renne, P.R., WoldeGabriel, G., Vrba, E.S., White, T.D., 2002. Remains of *Homo erectus* from Bouri, Middle Awash, Ethiopia. Nature 416, 317–320.

Asfaw, B., Gilbert, W.H., Richards, G.D., 2008. *Homo erectus* cranial anatomy. In: Gilbert, W.H., Asfaw, B.T. (Eds.), *Homo erectus*. Pleistocene Evidence from the Middle Awash, Ethiopia. University of California Press, Berkeley, pp. 265–328.

Athreya, S., 2009. A comparative study of frontal bone morphology among Pleistocene hominin fossil groups. J. Hum. Evol. 57, 786–804.

Baab, K.L., 2007. Cranial shape variation in *Homo erectus*. Ph.D. Dissertation, City University of New York.

Baab, K.L., 2008a. A re-evaluation of the taxonomic affinities of the early *Homo* cranium KNM-ER 42700. J. Hum. Evol. 55, 741–746.

Baab, K.L., 2008b. The taxonomic implications of cranial shape variation in *Homo erectus*. J. Hum. Evol. 54, 827–847.

Baab, K.L., 2010. Cranial shape in Asian *Homo erectus*: geographic, anagenetic, and size-related variation. In: Norton, C.J., Braun, D.R. (Eds.), Asian Paleoanthropology: From Africa to China and Beyond. Springer, New York, pp. 57–79.

Baab, K.L., Freidline, S.E., Wang, S.L., Hanson, T., 2010. Relationship of cranial robusticity to cranial form, geography and climate in *Homo sapiens*. Am. J. Phys. Anthropol. 141.

Baab, K.L., McNulty, K.P., 2009. Size, shape, and asymmetry in fossil hominins: the status of the LB1 cranium based on 3D morphometric analyses. J. Hum. Evol. 57, 608–622.

Baab, K.L., McNulty, K.P., Harvati, K., 2013. *Homo floresiensis* contextualized: A geometric morphometric comparative analysis of fossil and pathological human samples. PLoS One 8, e69119.

Baab, K., 2014. Defining *Homo erectus*. In: Henke, W., Tattersall, I. (Eds.), Handbook of Paleoanthropology. Springer, Heidelberg, pp. 1–28.

Bauer, C.C., Harvati, K., 2015. A virtual reconstruction and comparative analysis of the KNM-ER 42700 cranium. Anat. Anzeiger 72, 129–140.

Black, D., 1929. Preliminary notice of the discovery of an adult *Sinanthropus* skull at Chou Kou Tien. Bull. Geol. Soc. China 8, 15–32.

Black, D., 1931. On an adolescent skull of *Sinanthropus pekinensis* in comparison with an adult skull of the same species and with other hominid skulls, recent and fossil. Paleont. Sin. New Ser. D 7, 1–144.

Bookstein, F.L., 2002. Creases as morphometric characters. In: MacLeod, N., Forey, P.L. (Eds.), Morphology, Shape, and Phylogeny. CRC Press, New York, pp. 139–174.

Bräuer, G., 2008. The origin of modern anatomy: by speciation or intraspecific evolution? Evol. Anthropol. 17, 22–37.

Bräuer, G., Schultz, M., 1996. The morphological affinities of the Plio-Pleistocene mandible from Dmanisi, Georgia. J. Hum. Evol. 30, 445–481.

Brown, P., Maeda, T., 2009. Liang Bua *Homo floresiensis* mandibles and mandibular teeth: A contribution to the comparative morphology of a new hominin species. J. Hum. Evol. 57, 571–596.

Brown, F.H., McDougall, I., 1993. Geologic setting and age, The Nariokotome *Homo erectus* Skeleton. Harvard University Press, Cambridge, pp. 9–20.

Bruner, E., Manzi, G., Arsuaga, J.L., 2003. Encephalization and allometric trajectories in the genus *Homo*: Evidence from the Neandertal and modern lineages. Proc. Natl. Acad. Sci. USA 100, 15335–15340.

Clark, R.J., 1976. New cranium of *Homo erectus* from Lake Ndutu, Tanzania. Nature 262, 485–487.

Conroy, G.C., Jolly, C.J., Cramer, D., Kalb, J.E., 1978. Newly discovered fossil hominid skull from the Afar depression, Ethiopia. Nature 475, 67–70.

Day, M.H., Stringer, C.B., 1982. A reconsideration of the Omo Kibish remains and the *erectus-sapiens* transition. In: de Lumley, M.-A. (Ed.), *Homo erectus* et la Place de l'Homme de Tautavel parmi les Hominidés Fossiles, Première Congrès International de Paléontolgie Humaine. UNESCO Colloque International du Centre National de la Recherche Scientifique, Vol. 2. Prétirages, Nice, pp. 814–846.

de Lumley, M.-A., Gabounia, L., Vekua, A., Lordkipandize, D., 2006. Les restes humains du Pliocène final et du début du Pléistocène inférieur de Dmanissi, Géorgie (1991-2000). I - Les crânes, D 2280, D 2282, D 2700. L'Anthropologie 110, 1–110.

Dean, M.C., Wood, B.A., 1982. Basicranial anatomy of Plio-Pleistocene hominids from East and South Africa. Am. J. Phys. Anthropol. 59, 157–174.

Dean, C., Leakey, M.G., Reid, D., Schrenk, F., Schwartz, G.T., Stringer, C., Walker, A., 2001. Growth processes in teeth distinguish modern humans from *Homo erectus* and earlier hominins. Nature 414, 628–631.

Delson, E., Harvati, K., Reddy, D., Marcus, L.F., Mowbray, K., Sawyer, G.J., Jacob, T., Marquez, S., 2001. The Sambungmacan 3 *Homo erectus* calvaria: A comparative morphometric and morphological analysis. Anat. Rec. 262, 380–397.

Dubois, E., 1894. *Pithecanthropus erectus*, Eine Menschenahnliche Uebergangsfom aus Java. Landes Druecherei, Batavia.

Dunsworth, H., Walker, A., 2002. Early genus *Homo*. In: Hartwig, W.C. (Ed.), The Primate Fossil Record. Cambridge University Press, Cambridge, pp. 419–456.

Durband, A., 2006. Craniometric variation within the Pleistocene of Java: the Ngawi 1 cranium. Hum. Evol. 21, 193–201.

Franciscus, R.G., Trinkaus, E., 1988. Nasal morphology and the emergence of *Homo erectus*. Am. J. Phys. Anthropol. 75, 517–527.

Freidline, S.E., Gunz, P., Janković, I., Harvati, K., Hublin, J.J., 2012. A comprehensive morphometric analysis of the frontal and zygomatic bone of the Zuttiyeh fossil from Israel. J. Hum. Evol. 62, 225–241.

Friess, M., 2003. An application of the relative warps analysis to problems in human paleontology-with notes on raw data quality. Image Anal. Stereol. 22, 63–72.

Gabounia, L., de Lumley, M.-A., Vekua, A., Lordkipanidze, D., de Lumley, H., 2002. Decouverte d'un nouvel hominide a Dmanissi (Transcaucasie, Georgie). C. R. Palevol. vol. 1, 243–253.

Gabunia, L., Vekua, A., Lordkipanidze, D., Swisher III, C.C., Ferring, R., Justus, A., Nioradze, M., Tvalchrelidze, M., Antón, S.C., Bosinski, G., 2000. Earliest Pleistocene hominid cranial remains from Dmanisi, Republic of Georgia: taxonomy, geological setting, and age. Science 288, 1019–1025.

Gilbert, W.H., White, T.D., Asfaw, B., 2003. *Homo erectus, Homo ergaster, Homo "cepranensis,"* and the Daka cranium. J. Hum. Evol. 45, 255–259.

Gilbert, W.H., Holloway, R.L., Kubo, D., Kono, R.T., Suwa, G., 2008. Tomographic analysis of the Daka calvaria. In: Gilbert, W.H., Asfaw, B. (Eds.), *Homo erectus*: Pleistocene Evidence from the Middle Awash, Ethiopia. University of California Press, Berkeley, pp. 329–347.

Gómez-Robles, A., Olejniczak, A.J., Martinón-Torres, M., Prado-Simón, L., Bermúdez de Castro, J.M., 2011. Evolutionary novelties and losses in geometric morphometrics: a practical approach through hominin molar morphology. Evolution 65, 1772–1790.

Graves, R.R., Lupo, A.C., McCarthy, R.C., Wescott, D.J., Cunningham, D.L., 2010. Just how strapping was KNM-WT 15000? J. Hum. Evol. 59, 542–554.

Gunz, P., Bookstein, F.L., Mitteroecker, P., Stadlmayr, A., Seidler, H., Weber, G.W., 2009. Early modern human diversity suggests subdivided population structure and a complex out-of-Africa scenario. Proc. Natl. Acad. Sci. 106, 6094–6098.

Holloway, R.L., 1975. Early hominid endocasts: volumes, morphology and significance for hominid evolution. In: Tuttle, R. (Ed.), Primate Functional Morphology and Evolution. Mouton, The Hague, pp. 393–416.

Holloway, R.L., 1978. Problems of brain endocast interpretation and African hominid evolution. In: Jolly, C. (Ed.), Early Hominids of Africa. Duckworth, London, pp. 379–401.

Holloway, R.L., 1981. The Indonesian *Homo erectus* brain endocasts revisited. Am. J. Phys. Anthropol. 55, 503–521.

Howell, F.C., 1978. Hominidae. In: Maglio, V.J., Cooke, H.B.S. (Eds.), Evolution of African Mammals. Harvard University Press, Cambridge, pp. 154–248.

Howell, F.C., 1999. Paleo-demes, species clades, and extinctions in the Pleistocene hominin record. J. Anthropol. Res. 55, 191–243.

Howells, W.W., 1980. *Homo erectus*—who, when and where: a survey. Yearb. Phys. Anthropol. 23, 1–23.

Hublin, J.-J., 1985. Human fossils from the North African Middle Pleistocene and the origin of *Homo sapiens*. In: Delson, E. (Ed.), Ancestors: The Hard Evidence. Alan R. Liss, New York, pp. 283–288.

Hublin, J.-J., 2001. Northwestern African Middle Pleistocene hominids and their bearing on the emergence of *Homo sapiens*. In: Barnham, L., Robson-Brown, K. (Eds.), Human Roots: Africa and Asia in the Middle Pleistocene. Western Academic and Specialist Press Limited, Bristol, pp. 99–121.

Hyodo, M., Matsu'ura, S., Kamishima, Y., Kondo, M., Takeshita, Y., Kitaba, I., Danhara, T., Aziz, F., Kurniawan, I., Kumai, H., 2011. High-resolution record of the Matuyama–Brunhes transition constrains the age of Javanese *Homo erectus* in the Sangiran dome, Indonesia. Proc. Natl. Acad. Sci. 108, 19563–19568.

Jacob, T., 1975. Morphology and paleoecology of early man in Java. In: Tuttle, R.H. (Ed.), Paleoanthropology: Morphology and Paleoecology. Mouton, The Hague, pp. 311–325.

Jaeger, J.J., 1975. Découverte d'un crâne d'hominidé dans le Pleistocène moyen du Maroc. In: Sigmon, B.A., Cybulski, J.S. (Eds.), Problèmes Actuels de Paléontologie-Evolution des Vertébrés. C.N.R.S, Paris, pp. 897–902.

Kaifu, Y., Baba, H., Aziz, F., 2006. Indonesian *Homo erectus* and modern human origins in Australasia: New evidence from the Sambungmacan Region, Central Java. Natl. Sci. Mus. Monogr. 34, 289–294.

Kaifu, Y., Aziz, F., Indriati, E., Jacob, T., Kurniawan, I., Baba, H., 2008. Cranial morphology of Javanese *Homo erectus*: New evidence for continuous evolution, specialization, and terminal extinction. J. Hum. Evol. 55, 551–580.

Kidder, J.H., Durband, A.C., 2000. The question of speciation in *Homo erectus* revisited I: the metric evidence. Am. J. Phys. Anthropol. 30, 194–195.

Kidder, J.H., Durband, A.C., 2004. A re-evaluation of the metric diversity within *Homo erectus*. J. Hum. Evol. 46, 299–315.

Klingenberg, C.P., 2008. Novelty and "homology-free" morphometrics: What's in a name? Evol. Biol. 35, 186–190.

Kramer, A., 1993. Human taxonomic diversity in the Pleistocene: does *Homo erectus* represent multiple hominid species? Am. J. Phys. Anthropol. 91, 161–171.

Lahr, M.M., 1996. The Evolution of Modern Human Diversity: A Study of Cranial Variation. Cambridge University Press, Cambridge.

Larick, R., Ciochon, R.L., Zaim, Y., Sudijono, Suminto, Rizal, Y., Aziz, F., Reagan, M., Heizler, M., 2001. Early Pleistocene 40Ar/39Ar ages for Bapang Formation hominins, Central Jawa, Indonesia. Proc. Natl. Acad. Sci. 98, 4866–4871.

Le Gros Clark, W.E., 1940. The relationship between *Pithecanthropus* and *Sinanthropus*. Nature 145, 70–71.

Le Gros Clark, W.E., 1955. The Fossil Evidence for Human Evolution. University of Chicago Press, Chicago.

Le Gros Clark, W.E., 1959. The crucial evidence for human evolution. Am. Scientist 47, 250A–252A, 299-313.

Lieberman, D.E., McBratney, B.M., Krovitz, G., 2002. The evolution and development of cranial form in *Homo sapiens*. Proc. Natl. Acad. Sci. USA 99, 1134–1139.

Lordkipanidze, D., Vekua, A., Ferring, R., Rightmire, G.P., Zollikofer, C.P., Ponce de León, M.S., Agusti, J., Kiladze, G., Mouskhelishvili, A., Nioradze, M., 2006. A fourth hominin skull from Dmanisi, Georgia. Anat. Rec. 288, 1146–1157.

Lordkipanidze, D., Ponce de León, M.S., Margvelashvili, A., Rak, Y., Rightmire, G.P., Vekua, A., Zollikofer, C.P.E., 2013. A complete skull from Dmanisi, Georgia, and the evolutionary biology of early *Homo*. Science 342, 326–331.

Macchiarelli, R., Bondioli, L., Chech, M., Coppa, A., Fiore, I., Rezene, R., Vecchi, F., Yosief, L., Rook, L., 2004. The late Early Pleistocene human remains from Buia, Danakil Depression, Eritrea. Riv. Ital. Paleontol. S. 110, 133–144.

MacIntosh, N.W.G., Larnach, S.L., 1972. The persistence of *Homo erectus* traits in Australian Aboriginal crania. Archaeol. Phys. Anthropol. Ocean 7, 1–7.

Mann, A., 1971. *Homo erectus*. In: Dolhinow, P., Sarich, V. (Eds.), Background for Man. Little, Brown, Boston.

Manzi, G., Bruner, E., Passarello, P., 2003. The one-million-year-old *Homo* cranium from Bouri (Ethiopia): a reconsideration of its *H. erectus* affinities. J. Hum. Evol. 44, 731–736.

Márquez, S., Mowbray, K., Sawyer, G., Jacob, T., Silvers, A., 2001. New fossil hominid calvaria from Indonesia—Sambungmacan 3. Anat. Rec. 262, 344–368.

Marítnez, I., Arsuaga, J.L., 1997. The temporal bones from Sima de los Huesos Middle Pleistocene site (Sierra de Atapuerca, Spain). A phylogenetic approach. J. Hum. Evol. 33, 283–318.

Martinón-Torres, M., Bermúdez de Castro, J.M., Gómez-Robles, A., Margvelashvili, A., Prado, L., Lordkipanidze, D., Vekua, A., 2008. Dental remains from Dmanisi (Republic of Georgia): Morphological analysis and comparative study. J. Hum. Evol. 55, 249–273.

Mbua, E., Bräuer, G., 2012. Patterns of Middle Pleistocene hominin evolution in Africa and the emergence of modern humans. In: Reynolds, S.C., Gallagher, A. (Eds.), African Genesis: Perspectives on Hominin Evolution. Cambridge University Press, New York, pp. 394–422.

McDougall, I., Brown, F.H., Fleagle, J.G., 2005. Stratigraphic placement and age of modern humans from Kibish, Ethiopia. Nature 433, 733–736.

Mitteroecker, P., Bookstein, F., 2011. Linear discrimination, ordination, and the visualization of selection gradients in modern morphometrics. Evol. Biol. 38, 100–114.

Mounier, A., Condemi, S., Manzi, G., 2011. The stem species of our species: A place for the archaic human cranium from Ceprano, Italy. PLoS ONE 6, e18821.

Oppenoorth, W.F.F., 1932a. Ein neuer diluvialer Urmensch von Java. Nat. u. Mus., Frankfort 62, 269–279.

Oppenoorth, W.F.F., 1932b. *Homo (Javanthropus) soloensis*, een pleistoceene mensch van Java. Wetesch Mededee. Dienst Mijnbauw Nederl Indie 20, 49–74.

Oppenoorth, W.F.F., 1937. The place of *Homo soloensis* among fossil men. In: MacCurdy, G.G. (Ed.), Early Man. J.B. Lipincott, Philadelphia, pp. 349–360.

Picq, P.G., 1990. L'articulation temporo-mandibulaire des hominidés. CNRS, Paris.

Polly, P.D., 2008. Developmental dynamics and G-matrices: Can morphometric spaces be used to model phenotypic evolution? Evol. Biol. 35, 83–96.

Qiu, Z.L., Gu, Y.Y., Zhang, Y.Y., Chang, S.S., 1973. Newly discovered *Sinanthropus* remains and stone artifacts at Choukoutien. Vertebrat. Palasiatic. 11, 109–131 (In Chinese).

Rightmire, G.P., 1984. Comparisons of *Homo erectus* from Africa and Southeast Asia. Cour. Foursch. Senck 69, 83–98.

Rightmire, G.P., 1988. *Homo erectus* and later Middle Pleistocene humans. Annu. Rev. Anthropol. 17, 239–259.

Rightmire, G.P., 1990. The Evolution of *Homo erectus*: Comparative Anatomical Studies of an Extinct Human Species. Cambridge University Press, Cambridge.

Rightmire, G.P., 1996. The human cranium from Bodo, Ethiopia: evidence for speciation in the Middle Pleistocene? J. Hum. Evol. 31, 21–39.

Rightmire, G.P., 1998. Evidence from facial morphology for similarity of Asian and African representatives of *Homo erectus*. Am. J. Phys. Anthropol. 106, 61–85.

Rightmire, G.P., 2007. Later Middle Pleistocene *Homo*. In: Henke, W., Tattersall, I. (Eds.), Handbook of Paleoanthropology. Springer-Verlag, Berlin, pp. 1695–1715.

Rightmire, G.P., 2008. *Homo* in the Middle Pleistocene: Hypodigms, variation, and species recognition. Evol. Anthropol. 17, 8–21.

Rightmire, G.P., 2009. Middle and later Pleistocene hominins in Africa and Southwest Asia. Proc. Natl. Acad. Sci. 106, 16046–16050.

Rightmire, G.P., 2013. *Homo erectus* and Middle Pleistocene hominins: Brain size, skull form, and species recognition. J. Hum. Evol. 65, 223–252.

Rightmire, G.P., Lordkipanidze, D., Vekua, A., 2006. Anatomical descriptions, comparative studies and evolutionary significance of the hominin skulls from Dmanisi, Republic of Georgia. J. Hum. Evol. 50, 115–141.

Rohlf, F.J., Slice, D., 1990. Extensions of the Procrustes method for the optimal superimposition of landmarks. System. Zool. 39, 40–59.

Rosas, A., Bermudez De Castro, J.M., 1998. On the taxonomic affinities of the Dmanisi mandible (Georgia). Am. J. Phys. Anthropol. 107, 145–162.

Santa Luca, A., 1980. The Ngandong Fossil Humans: A Comparative Study of a Far Eastern *Homo erectus* Group. Yale University Press, New Haven.

Sartono, S., 1991. A new *Homo erectus* skull from Ngawi, east Java. Indo-Pacific Prehistory Association Bulletin 11, 14–22.

Schwartz, J.H., 2004. Getting to know *Homo erectus*. Science 305, 53–54.

Spoor, F., Leakey, M.G., Gathogo, P.N., Brown, F.H., Antón, S.C., McDougall, I., Kiarie, C., Manthi, F.K., Leakey, L.N., 2007. Implications of new early *Homo* fossils from Ileret, east of Lake Turkana, Kenya. Nature 448, 688–691.

Spoor, F., Leakey, M.G., Antón, S.C., Leakey, L.N., 2008. The taxonomic status of KNM-ER 42700: A reply to Baab (2008a). J. Hum. Evol. 55, 747–750.

Stringer, C.B., 1984. The definition of *Homo erectus* and the existence of the species in Africa and Europe. Cour. Foursch. Senck 69, 131–143.

Stringer, C., 2012. The status of *Homo heidelbergensis* (Schoetensack 1908). Evol. Anthropol. 21, 101–107.

Switek, B., Oct. 17, 2013. Beautiful skull spurs debate on human history. National Geographic. http://news.nationalgeographic.com/news/2013/10/131017-skull-human-origins-dmanisi-georgia-erectus/. Accessed on: Dec. 12, 2014.

Terhune, C.E., Deane, A.S., 2008. Temporal squama shape in fossil hominins: relationships to cranial shape and a determination of character polarity. Am. J. Phys. Anthropol. 137, 397–411.

Terhune, C.E., Kimbel, W.H., Lockwood, C.A., 2007. Variation and diversity in *Homo erectus*: a 3D geometric morphometric analysis of the temporal bone. J. Hum. Evol. 53, 41–60.

Tobias, P.V., 1991. Olduvai Gorge: The Skulls, Endocasts and Teeth of *Homo habilis*, Volume 4. Cambridge University Press, Cambridge.

Trinkaus, E., 2006. Modern human versus Neandertal evolutionary distinctiveness. Curr. Anthropol. 47, 597–620.

Turner, A., Chamberlain, A., 1989. Speciation, morphological change and the status of African *Homo erectus*. J. Hum. Evol. 18, 115–130.

Vekua, A., Lordkipanidze, D., Rightmire, G.P., Agusti, J., Ferring, R., Maisuradze, G., Mouskhelishvili, A., Nioradze, M., De Leon, M.P., Tappen, M., Tvalchrelidze, M., Zollikofer, C., 2002. A new skull of early *Homo* from Dmanisi, Georgia. Science 297, 85–89.

Villmoare, B., 2005. Metric and non-metric randomization methods, geographic variation, and the single-species hypothesis for Asian and African *Homo erectus*. J. Hum. Evol. 49, 680–701.

von Cramon-Taubadel, N., 2009. Congruence of individual cranial bone morphology and neutral molecular affinity patterns in modern humans. Am. J. Phys. Anthropol. 140, 205–215.

Weidenreich, F., 1940. The torus occipitalis and related structures and their transformations in the course of human evolution. Bull. Geolog. Soc. China 19, 479–558.

Weidenreich, F., 1943. The skull of *Sinanthropus pekinensis*: a comparative study on a primitive hominid skull. Paleont. Sin. New Ser. D 10, 1–298.

Weidenreich, F., 1951. Morphology of Solo man. Anthropol. Pap Am. Mus. 43, 222–288.

Widianto, H., Grimaud-Herve, D., Sartono, S., 2001. The evolutionary position of the Ngawi calvaria. Indo-Pacific Prehistory Association Bulletin 21, 162–169.

Widianto, H., Zeitoun, V., 2003. Morphological description, biometry and phylogenetic position of the skull of Ngawi 1 (East Java, Indonesia). Int. J. Osteoarch. 13, 339–351.

Wolpoff, M.H., Thorne, A.G., Jelínek, J., Zhang, Y., 1994. The case for sinking *Homo erectus*. 100 years of *Pithecanthropus* is enough! Cour. Foursch. Senck 171, 341–361.

Wood, B.A., 1984. The origin of *Homo erectus*. Cour. Foursch. Senck 69, 111.

Wood, B.A., 1991. Koobi Fora Research Project: Hominid Cranial Remains. Oxford University Press, New York.

Wood, B.A., 1994. Taxonomy and evolutionary relationships of *Homo erectus*. Cour. Foursch. Senck 171, 159–165.

Wood, B., 2011. Did early *Homo* migrate "out of" or "in to" Africa? Proc. Natl. Acad. Sci. 108, 10375–10376.

Zeitoun, V., Détroit, F., Grimaud-Hervé, D., Widianto, H., 2010. Solo man in question: Convergent views to split Indonesian *Homo erectus* in two categories. Quatern. Int. 223–224, 281–292.